

Discovery of 3-Cyclopropylmethyl-7-(4-phenylpiperidin-1-yl)-8-trifluoromethyl[1,2,4]triazolo[4,3-*a*]pyridine (JNJ-42153605): A Positive Allosteric Modulator of the Metabotropic Glutamate 2 Receptor

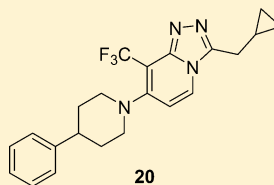
Jose María Cid,^{*,†} Gary Tresadern,[‡] Juan Antonio Vega,[†] Ana Isabel de Lucas,[†] Encarnación Matesanz,[†] Laura Iturrino,[†] María Lourdes Linares,[†] Aránzazu García,[†] José Ignacio Andrés,[†] Gregor J. Macdonald,[§] Daniel Oehlich,[§] Hilde Lavreysen,^{||} Anton Megens,^{||} Abdellah Ahnaou,^{||} Wilhelmus Drinkenburg,^{||} Claire Mackie,[⊥] Stefan Pype,[#] David Gallacher,[∞] and Andrés A. Trabanco[†]

[†]Neuroscience Medicinal Chemistry and [‡]Molecular Sciences, Janssen Research & Development, Janssen-Cilag S.A., Jarama 75, 45007 Toledo, Spain

[§]Neuroscience Medicinal Chemistry, ^{||}Neuroscience Biology, [⊥]Discovery ADME/Tox, [#]Project Management Office, and [∞]Center of Excellence for Cardiovascular Safety Research & Mechanistic Pharmacology, Janssen Research & Development, Turnhoutseweg 30, B-2340, Beerse, Belgium

S Supporting Information

ABSTRACT: Advanced leads from a series of 1,2,4-triazolo[4,3-*a*]pyridines with mGlu2 receptor PAM activity are reported. By modification of the analogous imidazo[1,2-*a*]pyridine series, the newly reported leads have improved potency, in vitro ADMET, and hERG as well as good in vivo PK profile. The optimization of the series focused on improving metabolic stability while controlling lipophilicity by introducing small modifications to the scaffold substituents. Analysis of this series combined with our previously reported mGlu2 receptor PAMs showed how lipophilic ligand efficiency was improved during the course of the program. Among the best compounds, example **20** (JNJ-42153605) showed a central in vivo efficacy by inhibition of REM sleep state at a dose of 3 mg/kg po in the rat sleep–wake EEG paradigm, a phenomenon shown earlier to be mGlu2 mediated. In mice, compound **20** reversed PCP-induced hyperlocomotion with an ED₅₀ of 5.4 mg/kg sc, indicative of antipsychotic activity.



mGlu2 PAM EC₅₀ = 17 nM
mGlu2 PAM E_{MAX} (%) = 285

in vivo active: sw-EEG at 3 mg/kg p.o.

PCP-LMA at 5.4 mg/kg s.c.

I INTRODUCTION

Glutamate is considered the major excitatory neurotransmitter in the mammalian central nervous system (CNS) of vertebrates, contributing excitatory input to as many as half of all central synapses. It plays a major role in numerous physiological functions such as learning and memory but also sensory perception, development of synaptic plasticity, motor control, respiration, and regulation of cardiovascular function. An imbalance in glutamatergic neurotransmission is believed to be at the center of various neurological and psychiatric diseases.^{1–7} Glutamate acts via activation of ionotropic or metabotropic glutamate receptors (iGlu or mGlu). The former includes ion channels such as NMDA, AMPA, and kainate receptors responsible for fast excitatory transmission, whereas the latter are a family of eight class C G-protein-coupled receptors contributing to the fine-tuning of synaptic efficacy.^{1,8,9} Glutamate activates mGlu receptors through binding at an orthosteric site in the amino terminal domain. This induces a conformational change in the receptor, resulting in activation of the G-protein and intracellular signaling pathways.¹⁰

The eight mGlu receptors are classified into three groups based upon sequence homology, pharmacological profile, and preferential signal transduction pathway.^{11,12} The mGlu2 receptor, which belongs to the group II subfamily along with mGlu3, has proven to be of particular importance in neuropharmacology. Preferentially expressed on presynaptic nerve terminals mGlu2 receptor negatively modulates glutamate and GABA release and is widely distributed in the brain.¹³ High levels of mGlu2 receptors are seen in brain areas such as prefrontal cortex, hippocampus, and amygdala where glutamate hyperfunction may be implicated in disorders and diseases such as anxiety and schizophrenia.^{14–17} It is therefore considered that activation of group II mGlu receptors may offer anxiolytic and/or antipsychotic effects.^{2,4,18}

The first generation pharmacological tools were conformationally constrained analogues of glutamate acting as agonists at both mGlu2 and mGlu3 receptors.¹⁹ Preclinical studies performed with mGlu2/3 receptor agonists such as (+)-2-aminobicyclo[3.1.0]hexane-2,6-dicarboxylic acid (LY354740)

Received: July 23, 2012

Published: October 16, 2012

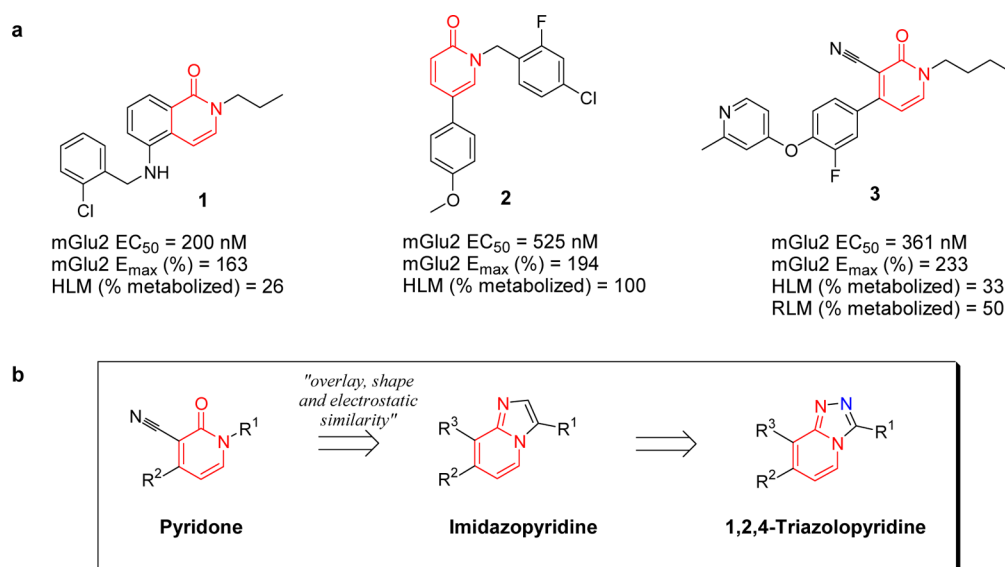


Figure 1. (a) Structures of mGlu2 PAM reported molecules (1–3). (b) Evolution from pyridone series to 1,2,4-triazolopyridine series.

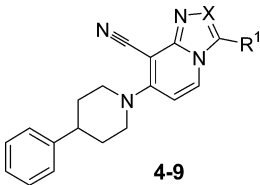
showed robust anxiolytic-like²⁰ and antipsychotic-like effects in animal models.²¹ Clinical data strengthen the rationale for group II receptor intervention as a treatment for schizophrenia. (1*R*,4*S*,5*S*,6*S*)-2-Thiabicyclo[3.1.0]hexane-4,6-dicarboxylic acid 4-[(2*S*)-2-amino-4-(methylthio)-1-oxobutyl]amino-2,2-dioxide monohydrate (LY2140023), the oral prodrug of the mGlu2/3 agonist (–)-(1*R*,4*S*,5*S*,6*S*)-4-amino-2-sulfonylbicyclo[3.1.0]hexane-4,6-dicarboxylic acid (LY404039), showed improvement of both positive and negative symptoms in schizophrenia in a double-blind placebo-controlled study in schizophrenic patients.²² Importantly, treatment with LY2140023 was safe and well-tolerated. It did not affect prolactin levels nor induce extrapyramidal symptoms or weight gain, in contrast to many of the current atypical antipsychotic medications.²³

Given the promise offered by mGlu2 receptor activation, there is increased interest in identifying small molecules that activate the receptor. A preferred approach is via positive allosteric modulators (PAMs) that bind at an alternative site to orthosteric agonists. This strategy offers many potential benefits: avoidance of amino acid like motifs that can be detrimental for CNS penetration, opportunity for greater chemical diversity, potential for improved selectivity, as the orthosteric site is highly conserved, and reduced likelihood of receptor desensitization, as PAMs typically activate the receptor only in the presence of glutamate and will respond to physiological neurotransmitter fluctuations.^{24–26} The number of reports on mGlu2 receptor PAM chemical series has increased over the past years.²⁷ Within our laboratories we have pursued a series of isoquinolones^{28,29} and 1,5-pyridones^{30,31} (1 and 2, respectively, Figure 1a). Those compounds were reported to be selective and moderately potent mGlu2 receptor PAMs; however, balancing potency and metabolic stability remained a challenge. We have very recently reported structurally related 3-cyanopyridones (3, Figure 1a).^{32–34} This scaffold delivered compounds with improved potency and druglike properties, and the latest results will soon be reported elsewhere.

These 3-cyanopyridone series were derived from HTS performed at the start of our program. However, with a need to expand the SAR, identify new chemotypes, and also gain more insight on the target, molecular modeling approaches

were employed to help identify and prioritize new chemical scaffolds. An overlay model revealed shared pharmacophoric features between reported series which were expected to be required for alternative motifs. On the basis of this model and methods of shape and electrostatic similarity, a novel series of imidazopyridines^{35–38} was discovered. The imidazopyridine serves as a surrogate for the pyridone core, in which the oxygen lone pair is replaced by a nitrogen lone pair of the imidazole ring, the ring centers of pyridone and pyridine overlap well, and the pendent groups are distributed along a similar vector. The series proved capable of delivering compounds with appealing pharmacological profile. However, exploration was mainly limited to compounds having trifluoroethyl as R¹ (Figure 1b), which was one of the few groups conferring acceptable potency and metabolic stability. Therefore, we considered improving metabolic stability by reducing lipophilicity with the introduction of an additional nitrogen atom, causing little disruption to overall molecular shape and features. This delivered the new 1,2,4-triazole template, which is the subject of this report (Figure 1b).

First, to test the viability of the imidazopyridine to triazolopyridine swap hypothesis, an initial set of imidazopyridines (4, 6, and 8) and their corresponding 1,2,4-triazolo[4,3-*a*]pyridines pairs (5, 7, and 9) were prepared (Table 1). In this set of compounds, both phenylpiperidine and cyano were selected as the most suitable substitutions to allow complete comparisons across the series. The reduction of the lipophilicity in the triazolopyridines did indeed correlate with an improvement of the metabolic stability of the compounds in both human and rat species. Interestingly, the *in vitro* potency was also retained. Herein we report the synthesis and structure–activity relationship (SAR) development of novel triazolopyridines^{39–41} as the culmination of the exploration around the imidazopyridine series. This exploration led to the identification of 3-cyclopropylmethyl-7-(4-phenyl-piperidin-1-yl)-8-trifluoromethyl[1,2,4]triazolo[4,3-*a*]pyridine (JNJ-42153605, 20), one of the most potent and selective mGlu2 PAMs identified in our program. Compound 20 influenced rat sleep–wake organization by decreasing REM sleep and reversed PCP-induced locomotor activity in mice. Hence, compound 20 is seen as a powerful pharmacological tool to gain more insight on

Table 1. Comparative Data for a Representative Set of Imidazopyridines (4, 6, 8) and Triazolopyridines (5, 7, 9)


compd	X	R ¹	clogP	mGlu2 EC ₅₀ (nM) ^a	mGlu2 E _{max} (%) ^a	HLM (%) ^b	RLM (%) ^b
4	C	Et	4.41	501	225	74	82
5	N	Et	3.38	696	247	11	7
6	C	ⁿ Pr	4.49	155	254	74	81
7	N	ⁿ Pr	3.91	299	272	25	40
8	C	CH ₂ CF ₃	4.35	125	259	24	41
9	N	CH ₂ CF ₃	3.33	56	277	9	10

^aValues are the mean of at least two experiments. ^bHLM and RLM data refer to % of compound metabolized after incubation with human or rat liver microsomes for 15 min at 5 μM.

the target as well as a suitable candidate for further development.

CHEMISTRY

Triazolopyridines 5, 7, 9–28 were synthesized following the routes outlined in Schemes 1–5. For the exploration of the R¹ group in cyano substituted triazolopyridines (5, 7, 9–12), 3-cyano-2,4-dibromopyridine (29) was chosen as starting material. Reaction of 29 with 4-phenylpiperidine (30) yielded the C-4 substitution product 31 with complete regioselectivity. Treatment of 31 with hydrazine under microwave heating led to the key 2-pyridylhydrazine intermediate 32 (Scheme 1),

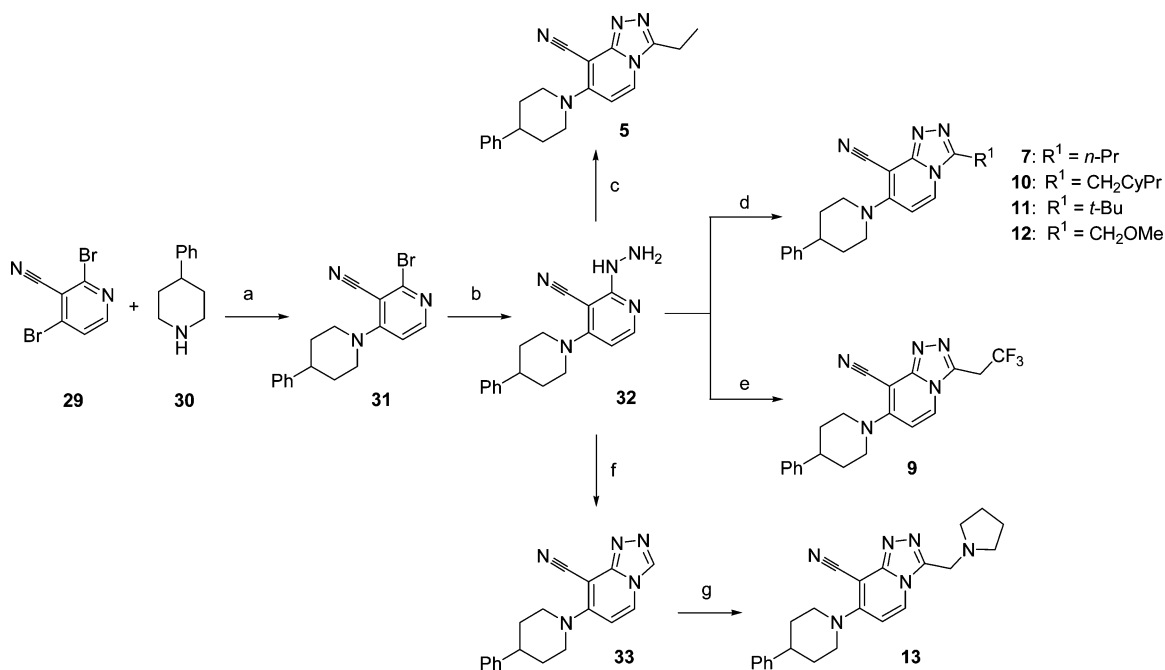
which was converted into the target 8-cyanotriazolopyridines by cyclization with several acid derivatives (orthoesters, acid chlorides, and carboxylic acids) under the reaction conditions shown in Scheme 1.

The triazolopyridines 14–17 substituted with a chlorine atom at position C-8 were prepared following a route similar to that described in Scheme 1. In this case, reaction of 2,3-dichloro-4-iodopyridine 34 with the piperidine derivatives 30 and 35 followed by nucleophilic substitution of the C-2 chlorine in 36a,b with hydrazine led to the 2-pyridylhydrazine derivatives 37a,b (Scheme 2). Subsequent cyclization of 37a,b with the corresponding acid derivatives resulted in the target molecules 14–17.

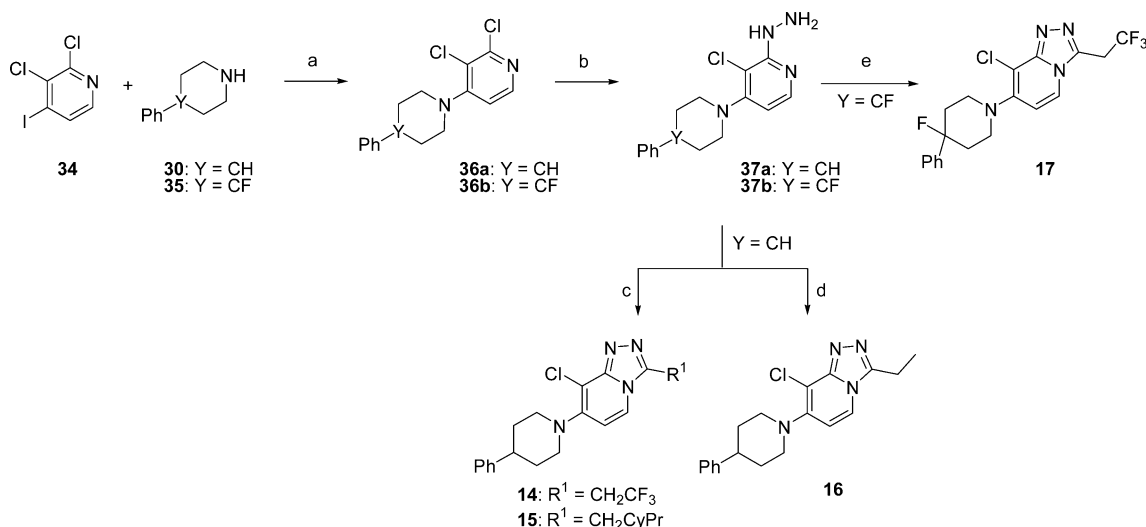
Derivatives 18 and 19 were prepared by Buchwald coupling of the corresponding amine (41³⁹ and 42) with the 8-chloro-7-iodotriazolopyridine 40 (Scheme 3). The synthesis of 40 was achieved in three steps by reaction of hydrazine with 34 followed by acylation and subsequent cyclodehydration of the formed intermediate 39.

The C-8 trifluoromethyl substituted triazolopyridines, bearing a cyclopropylmethyl substituent in the triazole ring (20, 24–28), were prepared as shown in Scheme 4. Chlorine displacement in 2,4-dichloro-3-trifluoromethylpyridine 43 with benzyl alcohol yielded 44 with complete regioselectivity. Introduction of hydrazine in 44 to give 45 followed by treatment with POCl₃ led to the 7-chlorotriazolopyridine 46. Nucleophilic substitution of the activated choro atom in 46 with several piperidines (30, 47, 48) and cyclic amines (R'R''NH = tetrahydroisoquinoline, dihydroisoindoline, and *rac*-3-phenylpyrrolidine) led to the target compounds 20 and 24–28.

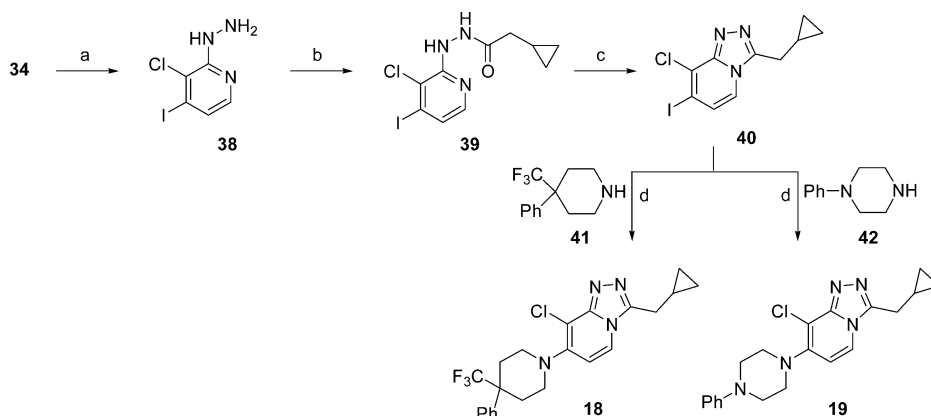
Finally, compounds 21–23 were obtained after nucleophilic substitution of 39 with the piperidines 30 and 35 followed by

Scheme 1^a

^aReagents and conditions: (a) NaH, DMF, rt, 1 h; (b) NH₂NH₂, THF, 160 °C, 15 min, microwave; (c) EtC(OEt)₃, xylenes, 180 °C, 2 h; (d) (i) R¹COCl, Et₃N, CH₂Cl₂ or CHCl₃, rt, 1–16 h; (ii) POCl₃, CH₃CN, 150 °C, 10 min, microwave; (e) CF₃CH₂CO₂H, DIPEA, CCl₃CN, PS-PPh₃, 1,2-dichloroethane, 150 °C, 18 min, microwave; (f) HC(OEt)₃, xylenes, 180 °C, 2 h; (g) CH₂O, pyrrolidine, AcOH, 80 °C, 16 h.

Scheme 2^a

^aReagents and conditions: (a) DIPEA, CH₃CN, 110 °C, 16 h; (b) NH₂NH₂, EtOH, 160 °C, 20 min, microwave; (c) (i) R¹COCl, Et₃N, CH₂Cl₂, rt, 1 h; (ii) POCl₃, CH₃CN, 150 °C, 10 min, microwave; (d) Et(OEt)₃, xylenes, 180 °C, 2 h; (e) (i) CF₃CH₂CO₂H, Et₃N, CH₂Cl₂, rt, 1 h; (ii) CCl₃CN, PS-Ph₃P, DIPEA, 1,2-dichloroethane, 100 °C, 16 h.

Scheme 3^a

^aReagents and conditions: (a) NH₂NH₂, 1,4-dioxane, 70 °C, 16 h; (b) CyPrCOCl, Et₃N, CH₂Cl₂, rt, 1 h; (c) 160 °C, 180 min; (d) Pd(AcO)₂, BINAP, Cs₂CO₃, toluene, 95 °C, 16 h.

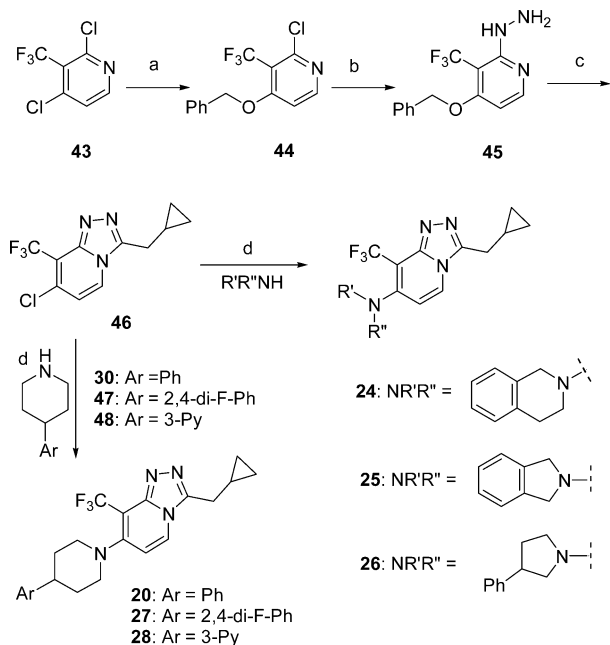
introduction of the hydrazine and standard cyclization processes with the corresponding acid derivatives.

RESULTS AND DISCUSSION

Representative compounds illustrating the SAR for this triazolopyridine series along with functional activity, metabolic stability, and hERG data are shown in Table 2. The triazolopyridine exploration began with the elaboration of the R¹ substitution. For these variations the cyano and phenylpiperidine substituents at R² and R³ were left constant (Table 2, compounds 5, 7, 9–13). Initial SAR showed that the R¹ substituent has an important effect on the potency (EC₅₀⁴²). Lengthening the alkyl chain from an ethyl to *n*-propyl led to a more than 2-fold increase in potency as exemplified with compounds 5 (696 nM) and 7 (299 nM). However, the increased size of the alkyl chain was detrimental for the metabolic stability in rat liver microsomes (RLMs) which increased from 7% (5) to 40% metabolized (7). A more balanced profile was found for compounds 9 and 10 which combined better metabolic stability with increased potency.

Interestingly, α -branching to the triazole ring was detrimental for mGlu2 PAM activity as shown with compound 11 (1230 nM). More diverse R¹ substitutions were explored as exemplified by the ether (12) and amine (13) analogues. These compounds, although metabolically stable, displayed decreased activity (468 nM for 12 and 1120 nM for 13). This suggests that polar groups are not well tolerated for activity in the R¹ region, which is in agreement with the moderate activity observed for compound 5 which has a less lipophilic R¹ alkyl chain. Of note, the cyanotriazolopyridines 5 and 9 showed weak inhibition of the hERG channel at 3 μ M in a patch clamp assay, 20% and 33%, respectively.

Next, our exploration focused on the R² substituent and was guided by SAR previously established for the imidazopyridine series.³⁵ In that case chlorine appeared to be beneficial for potency with an approximate 2-fold increase compared to the cyano group. The increase in activity correlated with the 0.9 log unit increase in lipophilicity by moving from cyano to chloro. This same approach was attempted in the triazolopyridine series; however, in this case the effect of the chlorine on the

Scheme 4^a

^aReagents and conditions: (a) BnOH, NaH, DMF, rt, 1 h; (b) NH₂NH₂, 1,4-dioxane, 160 °C, 30 min, microwave; (c) (i) CyPrCOCl, Et₃N, CH₂Cl₂, rt, 1 h; (ii) POCl₃, CH₃CN, 150 °C, 5 min, microwave; (d) amine, DIPEA, CH₃CN, 90–180 °C, 10 min to 24 h.

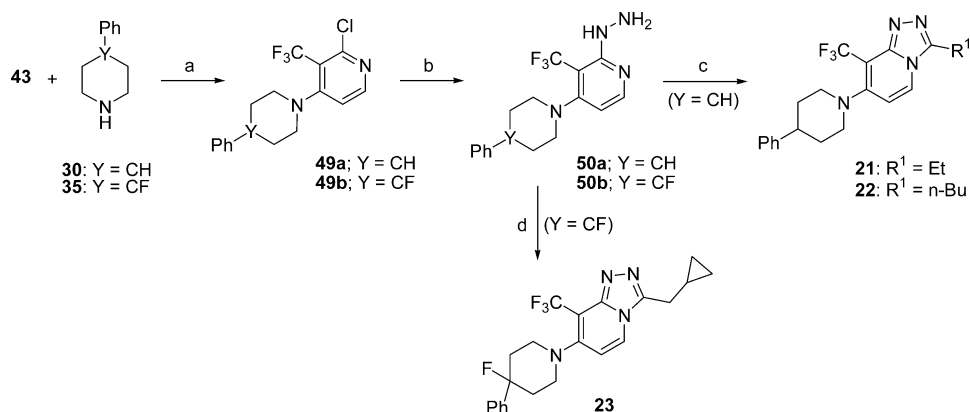
potency was not as consistent as for the imidazopyridine series. While the chloro analogue **16** showed a 2-fold increase compared to its cyano pair **5** (386 nM vs 696 nM, respectively), other chloro analogues (**14**, **15**) displayed potency comparable to that of their equivalent cyano versions (**9**, **10**). Unfortunately, chloro analogues were prone to be more metabolically unstable than cyano analogues. Furthermore, chlorine seemed to be detrimental for hERG liability (**16**, 43% vs **5**, 20% or **14**, 71% vs **9**, 33%), potentially a consequence of the increased lipophilicity.

Interestingly, the increase in hERG inhibition caused by the chlorine could be mitigated in some analogues by the introduction of additional groups at the 4-position of the 4-

piperidine. Thus, compound **17**, having a 4-fluoro-4-phenylpiperidine R² substituent, showed improvement of the hERG profile (**17**, 42% vs **14**, 71%). This 4,4-disubstitution of the piperidine ring also led to a 2-fold decrease in potency and slightly higher metabolic turnover. Nevertheless **17** was considered to have an overall better profile than **14**. The same trends were found with the 4-phenyl-4-trifluoromethylpiperidine analogue **18**, which also showed a remarkable reduction of hERG inhibition when compared to the corresponding pair **15** (**18**, 42% vs **15**, 99%). Although a similar 2-fold decrease in functional activity was found for **18**, its metabolic profile was similar to that of **15**. Replacement of the piperidine R² substituent by a piperazine led to a 9-fold decrease in mGlu2 PAM activity (**19**, 944 nM vs **15**, 102 nM).

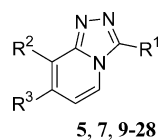
A breakthrough was achieved by the identification of the CF₃ group as an optimal replacement for the R² cyano and chloro substituents. A significant increase in potency was found over the R² cyano and chloro subclasses (**20** vs **10** or **15** and **21** vs **5** and **16**). In particular, compound **20** was found to be the most potent mGlu2 PAM identified so far, with an EC₅₀ of 17 nM and E_{max} of 285%.⁴³ This increase in potency promoted by the R² CF₃ substituent was consistent across several R¹ and R³ variations.^{39–41} In addition the positive effect of the CF₃ group was accompanied by acceptable metabolic stability and reduced hERG inhibition.

Fine tuning around the structure of **20** did not result in compounds with an improved profile. For instance, shorter (**21**) and longer (**22**) R¹ alkyl groups were tolerated in terms of potency and metabolic stability with the more lipophilic **22** being more potent than **21** (**21**, 116 nM; **22**, 24 nM). However, lengthening the alkyl chain had a detrimental effect on hERG inhibition (**20**, 56% vs **22**, 91%). Opposite the finding in the R³ chloro subclass (**17**), the introduction of fluorine at the C-4 position of the piperidine did not result in an improved hERG profile for the trifluoromethyltriazolopyridine **23** (**23**, 84% vs **20**, 57%). Fused variations of the 4-phenylpiperidine, such as **24** and **25**, turned out to be detrimental for activity (149 and 400 nM, respectively) as well as for metabolic stability. Ring contraction of the piperidine into pyrrolidine **26** led to an 80-fold drop in mGlu2 PAM potency together with worse metabolic stability. Finally, SAR on the aryl substituent of the piperidine ring in **20**

Scheme 5^a

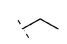
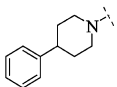
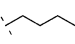
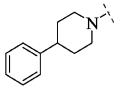

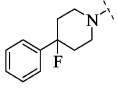
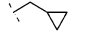
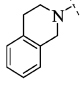
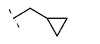
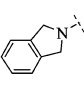
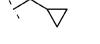
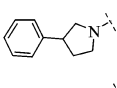

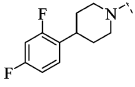
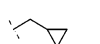
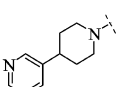
^aReagents and conditions: (a) **30**, NaH, DMF, rt, 1 h or **35**, DIPEA, CH₃CN, 110 °C, 4 h; (b) NH₂NH₂, THF, 160 °C, 45 min, microwave; (c) (i) R¹COCl, Et₃N, CH₂Cl₂, rt, 1 h; (ii) POCl₃, MeCN, 150 °C, 10 min; (d) (i) CyPrCOCl, Et₃N, CH₂Cl₂, rt, 1 h; (ii) CCl₃CN, PS-Ph₃P, PS-DIPEA, 1,2-dichloroethane, 150 °C, 10 min, microwave.

Table 2. Functional Activity, Metabolic Stability, and hERG Data of Representative mGlu2 Receptor PAMs 5, 7, 9–28



<i>Compd</i>	<i>R</i> ¹	<i>R</i> ²	<i>R</i> ³	<i>mGlu2</i> <i>EC</i> ₅₀ (nM) ^a	<i>mGlu2</i> <i>E</i> _{max} (%) ^a	<i>HLM</i> (%) ^b	<i>RLM</i> (%) ^b	<i>hERG</i> ^c
5		CN		696	247	11	7	20
7		CN		299	272	25	40	n.t. ^d
9		CN		56	277	9	10	33
10		CN		74	278	6	25	n.t. ^d
11		CN		1230	207	n.t. ^d	n.t. ^d	n.t. ^d
12		CN		468	196	12	31	n.t. ^d
13		CN		1120	240	38	88	n.t. ^d
14		Cl		55	300	13	8	71
15		Cl		102	343	56	n.t. ^d	99
16		Cl		386	262	57	39	43
17		Cl		116	310	39	25	42
18		Cl		178	243	56	41	43
19		Cl		944	308	62	53	n.t. ^d
20		CF ₃		17	285	23	25	57

Table 2. continued

Compd	R ¹	R ²	R ³	mGlu2 EC ₅₀ (nM) ^a	mGlu2 E _{max} (%) ^a	HLM (%) ^b	RLM (%) ^b	hERG ^c
21		CF ₃		116	334	29	42	36
22		CF ₃		24	364	33	54	91
23		CF ₃		39	292	18	13	84
24		CF ₃		149	278	52	86	n.t. ^d
25		CF ₃		400	330	50	89	n.t. ^d
26		CF ₃		1230	175	38	72	n.t. ^d
27		CF ₃		10	306	2	16	91
28		CF ₃		519	268	31	78	n.t. ^d

^aValues are the mean of at least two experiments. ^bHLM and RLM data refer to % of compound metabolized after 15 min at 5 μ M. ^cExperiments were performed using HEK293 cells stably transfected with the hERG potassium channel. Whole-cell currents were recorded with an automated patch-clamp system (PatchXpress 7000A). Three concentrations of compound were tested (0.1, 0.3, and 3 μ M; $n = 3$) and compared to vehicle (0.1% DMSO; $n = 3$). Data are presented as % inhibition at the highest concentration tested (3 μ M). ^dNot tested.

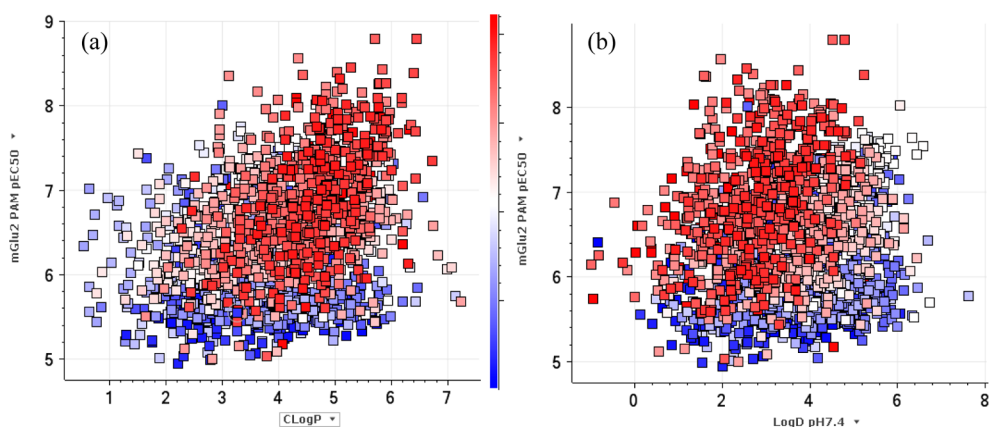


Figure 2. (a) mGlu2 PAM pEC₅₀ activity versus clogP (Biobyte). (b) mGlu2 PAM pEC₅₀ activity versus log *D* at pH 7.4 (ACD, version 12.0). Molecules are color-coded by order of registration in our internal database, the earliest compounds being blue and later compounds red. Plots combine data generated from several previously reported series: pyridones, isoquinolones, imidazopyridines, and triazolopyridines reported here. Inactive compounds for which exact pEC₅₀ could not be determined because of concentration limits were removed from the analysis.

is illustrated with compounds 27 and 28, showing that increased lipophilicity is well tolerated for activity (27, 10 nM) while detrimental for hERG inhibition (91%). Increased polarity such as in 28 led to compounds with decreased activity (28, 519 nM). In summary, a good understanding of the SAR and the effects of lipophilicity led to compounds with optimal

in vitro profile combining potency, metabolic stability in both human and rat species, and acceptable preliminary cardiovascular profile.

As discussed here and in recent articles describing other series,^{32,35,36} we have sought to balance primary in vitro activity and lipophilicity. The detrimental effects of increased lip-

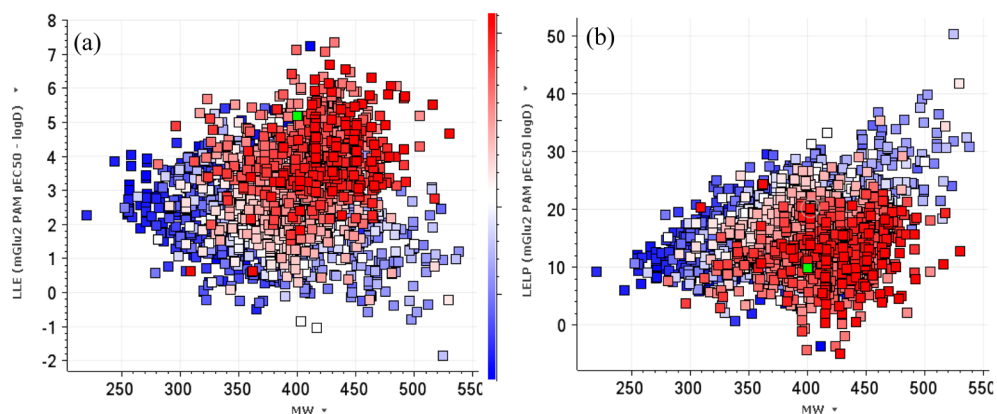


Figure 3. (a) Plot of LLE versus MW. (b) Plot of LELP versus MW. Molecules are color-coded by order of registration in our internal database, the earliest compounds being blue and later compounds red. Molecule **20** is highlighted in green. Plots combine data generated from several previously reported series: pyridones, isoquinolones, imidazopyridines, and triazolopyridines reported here. Inactive compounds for which exact pEC_{50} could not be determined because of concentration limits were removed from the analysis. To account for basic compounds, ACDLabs, version 12.0, $\log D$ at pH 7.4 was used for LLE and LELP calculations.

Table 3. Effect of CN, Cl, and CF_3 Substitution on Brain and Plasma Levels after 1 h of a Single Dose at 10 mg/kg in the Swiss Mouse

<i>Compd</i>	R^1	R^2	<i>Plasma levels</i> (ng/mL) ^a	<i>Brain levels</i> (ng/mL) ^a	<i>B/P ratio</i>	<i>cLogP</i> ^b	<i>TPSA</i>
5^c		CN	672	135	0.2	3.3	57
14^d		Cl	1162	2089	1.8	4.6	33
15^d		Cl	2661	3833	1.4	5.1	33
20^d		CF_3	671	849	1.3	5.3	33

^aData are expressed as the geometric mean values of at least two runs. ^b $\log P$ calculated with Biobyte software. ^cCompound dosed po in 0.5% Methocel suspension. ^dCompound dosed sc in 1 mg/mL in 20% HP- β -CD + HCl solution at pH 4.

ophilicity on many ADMET parameters⁴⁴ and druglikeness are well-known.⁴⁵ Figure 2 shows mGlu2 PAM pEC_{50} activity versus calculated $\log P$ and $\log D$ (pH 7.4) for molecules from multiple chemical series pursued within our mGlu2 PAM program. The plots include examples from previously reported pyridone, isoquinolone, and imidazopyridine series as well as the triazolopyridines reported herein. Such plots provide an interesting way to analyze compounds; for instance, those in the top left quadrant would be preferred because they are most active while having lower $\log P$. The molecules in Figure 2 are color-coded according to the rank order in which they were registered in our database, reflecting the progression of the project over time: blue being the oldest and red the newest registered compounds. As might be expected for small-molecule target interactions, $\log P$ shows a weak correlation with in vitro activity, with a Pearson correlation coefficient of 0.36 ($r^2 = 0.13$). This highlights the difficulty that was faced throughout the program to maintain lipophilicity in check. It can be seen that potency improved during the course of the program, with later compounds (red) generally having higher activity compared to earlier examples (blue). The Pearson correlation coefficient between the mGlu2 PAM pEC_{50} and compound registration rank order was 0.51. This is reflected in the SAR in Table 2, which shows more potent examples than

previously reported, for instance, compound **20**. It appears that later molecules, those colored red, have higher $\log P$, suggesting that improved potency arose at the cost of increased lipophilicity. However, among the more recent compounds there was a large set of intentionally designed basic molecules. Therefore, for this data set the calculated $\log D$ at pH 7.4 is a better measure for lipophilicity (Figure 2b). In this case, for compounds that were registered later $\log D$ values were lower, suggesting reduced apparent lipophilicity and a more optimal potency lipophilicity balance.

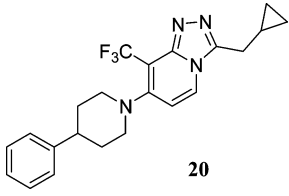
Parameters such as lipophilic ligand efficiency (LLE, pEC_{50} minus $\log D$)⁴⁵ and lipophilicity-corrected ligand efficiency (LELP, ratio $\log D/LE$)⁴⁶ have emerged as useful tools for lead optimization to address and monitor the lipophilicity and potency balance.⁴⁷ We examined how these parameters evolved for molecules synthesized during the project (Figure 3). Interestingly, both LLE and LELP improved over the course of the program with the newer molecules (red) tending to have higher LLE and lower LELP values. LLE values greater than 5 are typically preferred, and some of the later molecules reach such levels, with compound **20** having an LLE of 5.2.⁴⁸ LELP values, which are more suitable for optimization of fragments, are preferred to be lower. Although there are limitations for molecules with $\log D < 1$, it can be seen that there were many

Table 4. PK Data for Compounds 17, 18, 20, and 21 in Rat after Oral and Intravenous Administration^a

compd	Cl (mL min ⁻¹ kg ⁻¹) ^b	T _{1/2} (h) ^b	Vd _{ss} (L/kg) ^b	T _{max} (h) ^b	AUC _{0–inf} (ng·h/mL) ^b	C _{max} (ng/mL) ^b	F (%)	B/P ^c
17	18	2.6	1.9	1.7	5987	807	63	1.4
18	77	2.1	5.1	1.3	1159	289	53	1.6
20	35	2.7	1.4	0.5	1804	482	36	1.4
21	53	1.9	1.4	0.7	1009	359	35	1.3

^aStudy in male Sprague–Dawley rat dosed at 10 mg/kg po and 2.5 mg/kg iv, formulated in 20% HP-β-CD at pH 4. ^bValues are the mean of three animals. ^cRatios calculated after 1 h of a single dose at 10 mg/kg sc in 1 mg/mL in 20% HP-β-CD + HCl solution at pH 4 in the Swiss mouse.

Table 5. Overview of Compound 20

		20
physicochemical properties	MW = 440 exptl pK _a = 4.1 exptl log P = 4.4 at pH 7	
in vitro	mGlu2 PAM EC ₅₀ = 17 nM; E _{max} = 67% mGlu2 Ago EC ₅₀ = 270 nM; E _{max} = 285% mGlu2 PAM binding ⁵⁷ IC ₅₀ = 15 nM selectivity (mGlu1,3–8) of >100-fold vs mGlu2 PAM selectivity (CEREP) ⁴⁹ of >50-fold vs mGlu2 PAM	
ADME profile	solubility of <0.004 mg/mL in water and 0.995 mg/mL 20% HP-β-CD at pH 4 plasma protein binding (%) of 99.82 (h), 99.65 (r) metabolism (%) ^a of 23 (HLM), 25 (RLM) CYP450 inhibition of 1A2, 2D6, 3A4 (>30 μM), 2C9 (11 μM), 2C19 (20 μM) permeability (LLC-PK1 cells, ABCB1) AB/BA P _{app} × 10 cm s ⁻¹ = 12/6	
rat PK: 2.5 mg/kg iv, 10 mg/kg po	Cl = 35 mL min ⁻¹ kg ⁻¹ ; Vd _{ss} = 1.4 L/kg; T _{max} = 0.5 h; T _{1/2} = 2.7 h AUC _{0–inf} = 1804 ng·h/mL; C _{max} = 482 ng/mL; F = 35%; B/P = 1.4	
dog PK: 1 mg/kg iv, 2.5 mg/kg po	Cl = 29 mL min ⁻¹ kg ⁻¹ ; Vd _{ss} = 1.3 L/kg; T _{max} = 0.5 h; T _{1/2} = 0.8–1.1 h AUC _{0–inf} = 531–957 ng·h/mL; C _{max} = 218–472 ng/mL; F = 18–33%	
swEEG rat po	LAD = 3 mg/kg (free plasma concn of 0.14 ng/mL)	
PCP-LMA mice sc	ED ₅₀ = 5.4 mg/kg (free plasma concn of 2.6 ng/mL)	
CV safety	hERG PC (% inh at 3 μM) ^b = 57%; NOEL = 0.1 μM; margin = 285 ^d rabbit purkinje fiber; NOEL = 0.075 μM; margin = 214 ^d anesthetized guinea pig; NOEL = 9000 ng/mL; margin = 225 ^d anesthetized dog; NOEL = 6625 ng/mL; margin = 165 ^d	
genotoxicity	Ames TA98: ⁵⁸ clean up to 125 mg/mL in vitro micronucleus: ^c clean up to 150 μg/mL	

^aHLM and RLM data refer to % of compound metabolized after 15 min at 5 μM. ^bExperiments were performed using HEK293 cells stably transfected with the hERG potassium channel. Whole-cell currents were recorded with an automated patch-clamp system (PatchXpress7000A). Three concentrations of compound were tested (0.1, 0.3, and 3 μM; n = 3) and compared with vehicle (0.1% DMSO; n = 3). Data are presented as percent inhibition at the highest concentration tested (3 μM). ^cStudy conducted in human lymphoblastoid TK6 cell line in the presence or absence of metabolic activation (rat liver S9). ^dBased on efficacy free concentration in sw-EEG model (0.14 ng/mL).

compounds with preferred values less than 10; for instance, compound 20 had LELP of 9.8. The retrospective analysis of these parameters showing their improvement throughout lead optimization suggests that they can be useful for guiding medicinal chemistry decision making.

We next investigated the ability of a representative set of compounds to cross the blood–brain barrier (BBB). Plasma and brain levels measured 1 h after dosing at 10 mg/kg are listed in Table 3. The cyano subclass (5) was much less brain penetrant (B/P = 0.2) than chloro or CF₃ subclasses (6.5- to 9-fold higher B/P ratios for 14, 15, and 20). This improvement for the chloro and CF₃ subseries may well be explained by a reduction of the TPSA and/or higher lipophilicity as shown in Table 3.

To ascertain the druglike properties of the series, further in vivo PK work was conducted with the most promising compounds (17, 18, 20, and 21). Data for relevant PK parameters are shown in Table 4. The most optimal PK data were obtained for compounds 17 and 20 with moderate to good plasma exposures after oral (po) administration (AUC of 5987 and 1804 ng·h/mL, respectively) combined with acceptable intravenous (iv) PK parameters, resulting in moderate to good bioavailability (F). In contrast, compounds 18 and 21 had a less favorable PK, with higher clearance (Cl) after iv dosing and shorter half-lives (T_{1/2}) resulting in more limited plasma exposures.

On the basis of these results, compound 20 showed the best overall profile among all analogues prepared, combining an

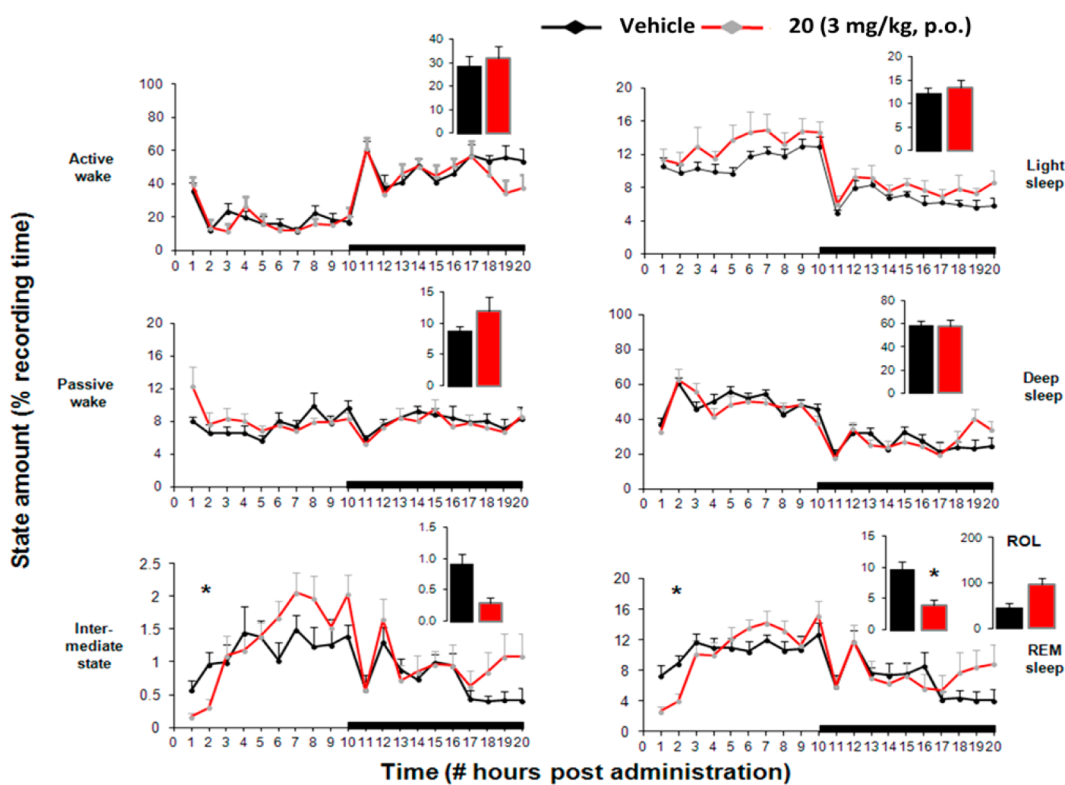


Figure 4. Effects of oral administration of **20** (3 mg/kg) or vehicle (20% CD + 2H2T) on sleep–wake organization in rats during 20 consecutive hours. Mean percentage of occurrence per minute is indicated for each sleep–wake state. Small bar charts indicate amounts of vigilance states in min (plus SEM) during the first 2 h postadministration: ROL, REM sleep onset latency; *, $p < 0.05$; Wilcoxon–Mann–Whitney rank sum tests compared with vehicle values.

excellent mGlu2 PAM activity (15 nM) with acceptable PK profile and brain penetration. In addition, **20** was assessed for its selectivity for the mGlu2 receptor (data shown in Table 5) and was found to not have agonist or antagonist activity toward other mGlu receptor subtypes up to 30 μM (>50-fold vs mGluR2) and also showed no or negligible affinity or activity at any of the targets in the CEREP⁴⁹ panel of receptors (>100-fold selectivity for mGlu2 receptor). Therefore, **20** is a selective mGlu2 receptor PAM. Altogether, compound **20** represented suitable candidate to progress to further studies including in vivo pharmacology.

The link between sleep abnormalities and neurological and psychiatric disorders is widely reported. For instance, disturbances in rapid eye movement (REM) sleep are frequently seen in patients with major depressive disorder, and many clinically effective antidepressants produce common changes in sleep pattern such as reduced REM sleep and REM sleep onset latency. Glutamate concentrations fluctuate across different vigilance states, suggesting that glutamate in the forebrain may play a role in the sleep process.⁵⁰ Given the relationship between the mechanism of sleep and glutamate signaling, sleep–wake neurophysiological measures can offer a highly reliable, sensitive, and translational index of brain activity and target engagement. We have previously shown that mGlu2 receptor activation with the agonist LY354740 and PAM 3'-[[2-cyclopentyl-6,7-dimethyl-1-oxo-2,3-dihydro-1H-inden-5-yl]oxy]methyl)biphenyl-4-carboxylic acid (BINA) elicited common changes in the rodent's sleep–wake pattern (i.e., selectively suppress REM sleep), which supports an important role for the mGlu2 receptor in the regulation of REM sleep⁵¹ and that combining both compounds produces synergistic

effects. Subsequently we reported similar results for examples from our 1,4-pyridone and imidazopyridine series.^{32,36} In addition, reports from groups elsewhere confirm that mGlu2 activation by agonists or allosteric potentiators has consistent and robust effects seen in sleep–wake EEG.^{52–54} Therefore, we have evaluated the central activity of **20** in the sw-EEG paradigm, and the present results were in accordance with our earlier findings. Accordingly, **20** at a dose of 3 mg/kg (po) was centrally active and suppressed REM sleep during the first 2 h after administration without clear effects on the other sleep–wake stages (Figure 4, bottom right panel). In addition, **20** prolonged REM sleep onset latency (Figure 4, bottom right panel) whereas no indications of sleep fragmentation were revealed by examination of the total number of transitions from sleep states toward waking (data not shown). On the basis of plasma protein binding (data shown in Table 5), the active dose of 3 mg/kg po corresponded to an approximate free concentration in plasma of 0.14 ng/mL.⁵⁵

Compound **20** was further evaluated for its effect on phencyclidine-induced hyperlocomotion (PCP-LMA) in mice. The PCP-LMA model is based on the evidence that the noncompetitive NMDA receptor channel blocker phencyclidine (PCP) is capable of evoking schizophrenia-like symptoms in healthy subjects and worsens psychosis in schizophrenic patients,⁵⁶ and hence, PCP is widely used in animal models of psychosis. In rodents, PCP causes an increase in motor activity. As this induced behavior may be linked to increased glutamate release, it is speculated that mGlu2 receptor activation may block these specific PCP-mediated effects. Therefore, this represents a useful model of psychosis and serves as the basis for the “glutamate hypothesis of schizophrenia”. We have

administered **20** in mice pretreated with PCP and evaluated its effect on PCP-induced hyperlocomotion. As shown in Figure 5,

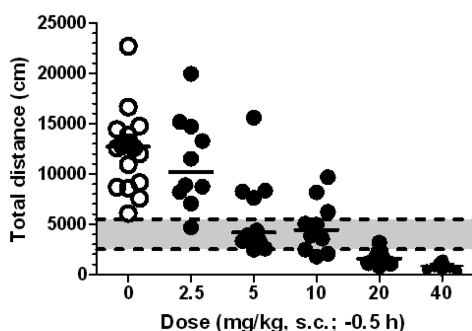


Figure 5. Effect of **20** on PCP-induced locomotor activity in mice. The gray horizontal bar represents the activity level measured in solvent treated control mice not challenged with PCP.

compound **20** dose-dependently and significantly attenuated the increase in locomotor activity induced by PCP (5 mg/kg sc) with an ED_{50} of 5.4 mg/kg sc which corresponded to an approximate free concentration in plasma of 2.6 ng/mL.⁵⁵

As shown in Table 5, **20** was extensively characterized for its ADMET and safety profile. Compound **20** has a low aqueous solubility (<0.004 mg/mL in water) which increases at pH \approx 4 and in complexation with cyclodextrines (0.995 mg/mL 20% HP- β -CD at pH 4).

Compound **20** showed a rapid rate of absorption from the gastrointestinal tract, reaching the maximal concentration after 0.5 h. Clearance in vivo was moderate to high in both rat and dog (35 and 29 mL min⁻¹ kg⁻¹, respectively). Elimination half-lives are on the shorter side across the species, being 2.7 h in rat and 0.8–1.1 h in dog. Volume of distribution is slightly higher than total body water, indicating distribution outside the plasma, which was confirmed in a rat tissue distribution study (data not shown). In vitro studies (LLC-PK1-MDR1) showed high permeability with no indication for P-glycoprotein (P-gp) efflux. Bioavailability is low to moderate across the species (35% in rat and 18–33% in dog). For a highly permeable compound, the low to moderate bioavailability might be related to an in vivo solubility/dissolution rate limiting factor that could reduce the extent of absorption.

Safety characterization of **20** did not reveal relevant alerts. Thus, compound **20** showed a low potential to inhibit the metabolism of co-medication (IC_{50} for five major CYP450 of >10 μ M; Table 5) and no genotoxic alerts based on both the Ames and the micronucleus tests.

Compound **20** displayed good safety margins in various cardiovascular studies. It did not affect IKr in hERG-transfected HEK293 cells at 0.1 μ M and did not induce electrophysiological effects in the isolated rabbit Purkinje fiber at \leq 0.075 μ M. This was more than 200-fold the estimated free efficacious plasma exposure of 0.14 ng/mL (taking into consideration the high plasma protein binding, i.e., 0.35% free). The no-effect levels (NOEL) in vivo (anesthetized guinea pigs and dogs, 9000 and 6625 ng/mL, respectively) are more than 160-fold the efficacious plasma exposure. On the basis of the currently available preclinical safety and efficacy data, the good safety margins attained support for further studies with compound **20**.

CONCLUSION

In summary, optimization of the previously reported imidazopyridine series led to the discovery of a novel series of 1,2,4-triazolo[4,3-*a*]pyridines. Lowering lipophilicity of the central core by the introduction of an additional nitrogen was key to delivering compounds with better metabolic stability while the potency remained comparable. These promising results were followed by sequential optimizations of hERG and PK profiles that led to compound **20** as the best triazolopyridine derivative identified. **20** turned out to be among the most potent mGlu2 receptor PAMs prepared so far, displaying very high in vitro potency of 17 nM and good selectivity for the mGlu2 receptor (>50-fold). Compound **20** showed an acceptable PK profile in rodent and non-rodent species. Likewise, it displayed good in vivo activity in models sensitive to mGlu2 modulation such as sw-EEG and PCP-LMA, both at doses remarkably better compared to leads previously reported in our program. Furthermore, there were no safety concerns identified that would hamper the progression of the compound. Collectively, compound **20** is considered a very attractive pharmacological agent to advance our knowledge of how mGlu2 receptor modulation may reduce the severity of diseases where disruption of glutamatergic transmission is pronounced and as an excellent candidate to progress toward clinical settings.

EXPERIMENTAL SECTION

Chemistry. Unless otherwise noted, all reagents and solvents were obtained from commercial suppliers and used without further purification. Thin layer chromatography (TLC) was carried out on silica gel 60 F254 plates (Merck). Flash column chromatography was performed on silica gel, particle size 60 Å, mesh of 230–400 (Merck) under standard techniques. Microwave assisted reactions were performed in a single-mode reactor, Biotage Initiator Sixty microwave reactor (Biotage), or in a multimode reactor, MicroSYNTH Labstation (Milestone, Inc.). Nuclear magnetic resonance (NMR) spectra were recorded with either a Bruker DPX-400 or a Bruker AV-500 spectrometer (Bruker AG) with standard pulse sequences, operating at 400 and 500 MHz, respectively, using CDCl₃ and DMSO-*d*₆ as solvents. Chemical shifts (δ) are reported in parts per million (ppm) downfield from tetramethylsilane (δ = 0). Coupling constants are reported in hertz. Splitting patterns are defined by s (singlet), d (doublet), dd (double doublet), t (triplet), q (quartet), quin (quintet), sex (sextet), sep (septet), or m (multiplet). Liquid chromatography combined with mass spectrometry (LCMS) was performed on either a HP 1100 HPLC system (Agilent Technologies) or Advanced Chromatography Technologies system composed of a quaternary or binary pump with degasser, an autosampler, a column oven, a diode array detector (DAD), and a column as specified in the respective methods below. Flow from the column was split to a MS spectrometer. The MS detector was configured with either an electrospray ionization source or an ESCI dual ionization source (electrospray combined with atmospheric pressure chemical ionization). Nitrogen was used as the nebulizer gas. Data acquisition was performed with MassLynx-Openlynx software or with Chemsation-Agilent data browser software. More detailed information about the different LCMS methods employed can be found in the Supporting Information. Melting point values are peak values and were obtained with experimental uncertainties that are commonly associated with this analytical method. Melting points were determined in open capillary tubes on a Mettler FP62 apparatus with a temperature gradient of 10 °C/min. Maximum temperature was 300 °C.

Purities of all new compounds were determined by analytical RP-HPLC using the area percentage method on the UV trace recorded at a wavelength of 254 nm, and compounds were found to have \geq 95% purity unless otherwise specified.

3-Ethyl-7-(4-phenylpiperidin-1-yl)[1,2,4]triazolo[4,3-*a*]pyridine-8-carbonitrile (5). A solution of **32** (0.05 g, 0.17 mmol) and EtC(OEt)₃ (0.46 mL, 2.56 mmol) in xylenes (1 mL) was heated in a sealed tube at 180 °C for 2 h. After the mixture was cooled to room temperature, the volatiles were evaporated in vacuo. The residue thus obtained was precipitated by treatment with Et₂O. The resulting solid was filtered off and dried in the vacuum oven (50 °C) to give **5** (0.042 g, 74%). ¹H NMR (500 MHz, CDCl₃) δ 1.31 (t, *J* = 7.5 Hz, 3 H), 1.77 (qd, *J* = 12.6, 3.8 Hz, 2 H), 1.95 (br d, *J* = 11.3 Hz, 2 H), 2.86–2.95 (m, 1 H), 3.00 (q, *J* = 7.5 Hz, 2 H), 3.34–3.42 (m, 2 H), 4.32 (br d, *J* = 13.3 Hz, 2 H), 6.96 (d, *J* = 7.8 Hz, 1 H), 7.19–7.25 (m, 1 H), 7.26–7.37 (m, 4 H), 8.34 (d, *J* = 8.1 Hz, 1 H). LCMS: *m/z* 332 [M + H]⁺, *t_R* = 3.46 min.

7-(4-Phenylpiperidin-1-yl)-3-propyl[1,2,4]triazolo[4,3-*a*]pyridine-8-carbonitrile (7). To a solution of **32** (0.2 g, 0.68 mmol) in dry CH₂Cl₂ (2 mL) cooled at 0 °C were added Et₃N (0.14 mL, 1.02 mmol) and butanoyl chloride (0.087 g, 0.82 mmol). The resulting reaction mixture was allowed to gradually warm to room temperature and then further stirred for 1 h. NaHCO₃ (aqueous saturated solution) was added, and the resulting solution was then extracted with CH₂Cl₂. The organic layer was separated, dried over MgSO₄, and the volatiles were evaporated in vacuo. The residue thus obtained was dissolved in 1,2-dichloroethane (2 mL), and POCl₃ (0.035 mL, 0.371 mmol) was added. The resulting mixture was heated at 150 °C for 5 min under microwave irradiation. After cooling to room temperature, the mixture was diluted with CH₂Cl₂ and washed with NaHCO₃ (aqueous saturated solution). The organic layer was separated, dried over Na₂SO₄, and concentrated in vacuo. The residue thus obtained was purified by column chromatography (silica gel, EtAcO in CH₂Cl₂, 0/100 to 40/50) to give **7** (0.039 g, 17%). Mp > 300 °C. ¹H NMR (400 MHz, CDCl₃) δ 1.05 (t, *J* = 7.4 Hz, 3 H), 1.81–1.98 (m, 4 H), 2.07 (br d, *J* = 12.0 Hz, 2 H), 2.84 (tt, *J* = 12.1, 3.5 Hz, 1 H), 2.97 (t, *J* = 7.5 Hz, 2 H), 3.38 (br t, *J* = 12.0 Hz, 2 H), 4.30 (br d, *J* = 13.2 Hz, 2 H), 6.60 (d, *J* = 7.9 Hz, 1 H), 7.20–7.29 (m, 3 H), 7.30–7.38 (m, 2 H), 7.75 (d, *J* = 7.9 Hz, 1 H). LCMS: *m/z* 346 [M + H]⁺, *t_R* = 3.03 min.

7-(4-Phenylpiperidin-1-yl)-3-(2,2,2-trifluoroethyl)[1,2,4]triazolo[4,3-*a*]pyridine-8-carbonitrile (9). To a suspension of **32** (0.3 g, 1.02 mmol) in dry CH₂Cl₂ (10 mL) at room temperature were added diisopropylethylamine (0.36 mL, 2.045 mmol), polymer supported PPh₃ (1.43 g, 3.07 mmol, loading 2.15 mmol/g), CF₃CO₂H (0.09 mL, 1.02 mmol), and trichloroacetonitrile (0.21 mL, 2.04 mmol) in 1,2-dichloroethane (10 mL). The resulting reaction mixture was heated at 150 °C under microwave irradiation for 18 min. After cooling to room temperature, the reaction mixture was filtered through a Celite pad and solids were washed thoroughly with CH₂Cl₂ and MeOH. The combined filtrates were concentrated in vacuo and the residue thus obtained was purified by column chromatography (silica gel, MeOH in CH₂Cl₂, 0/100 to 5/100) to give **9** (100 mg, 25%). Mp > 300 °C. ¹H NMR (500 MHz, CDCl₃) δ 1.92 (qd, *J* = 12.7, 3.8 Hz, 2 H), 2.09 (br d, *J* = 12.4 Hz, 2 H), 2.87 (tt, *J* = 12.1, 3.5 Hz, 1 H), 3.42 (br t, *J* = 12.7, 12.7 Hz, 2 H), 3.98 (q, *J* = 9.8 Hz, 2 H), 4.36 (br d, *J* = 13.3 Hz, 2 H), 6.70 (d, *J* = 7.8 Hz, 1 H), 7.21–7.26 (m, 3 H), 7.31–7.38 (m, 2 H), 7.86 (d, *J* = 7.8 Hz, 1 H). LCMS: *m/z* 386 [M + H]⁺, *t_R* = 3.82 min.

3-Cyclopropylmethyl-7-(4-phenyl-1-piperidin-1-yl)-1,2,4-triazolo[4,3-*a*]pyridine-8-carbonitrile (10). To a solution of **32** (0.8 g, 2.73 mmol) in dry CHCl₃ (14 mL) cooled at 0 °C were added Et₃N (0.61 mL, 4.36 mmol) and cyclopropylacetyl chloride (0.48 g, 4.09 mmol). The resulting reaction mixture was gradually warmed to room temperature and further stirred for 1 h. Then NaHCO₃ (aqueous saturated solution) was added, and the resulting solution was then extracted with CH₂Cl₂. The organic layer was separated, dried over MgSO₄, and concentrated in vacuo. The resulting residue was dissolved in 1,2-dichloroethane (10 mL), and POCl₃ (0.4 mL, 4.26 mmol) was added. The mixture was heated at 150 °C for 5 min under microwave irradiation. After cooling to room temperature, the mixture was diluted with CH₂Cl₂ and washed with NaHCO₃ (aqueous saturated solution). The organic layer was separated, dried over Na₂SO₄, and concentrated in vacuo. The residue thus obtained was purified by column chromatography (silica gel, MeOH–NH₃ in

CH₂Cl₂, 0/100 to 3/97) to give **10** (0.14 g, 15%). ¹H NMR (500 MHz, CDCl₃) δ 0.27–0.37 (m, 2 H), 0.56–0.69 (m, 2 H), 1.08–1.18 (m, 1 H), 1.85–1.98 (m, 2 H), 2.07 (br d, *J* = 11.6 Hz, 2 H), 2.85 (tt, *J* = 12.1, 3.5 Hz, 1 H), 3.00 (d, *J* = 6.6 Hz, 2 H), 3.39 (td, *J* = 12.8, 1.9 Hz, 2 H), 4.31 (br d, *J* = 13.3 Hz, 2 H), 6.61 (d, *J* = 7.8 Hz, 1 H), 7.22–7.27 (m, 3 H), 7.30–7.38 (m, 2 H), 7.85 (d, *J* = 7.8 Hz, 1 H). LCMS: *m/z* 358 [M + H]⁺, *t_R* = 3.88 min.

3-tert-Butyl-7-(4-phenyl-1-piperidin-1-yl)-1,2,4-triazolo[4,3-*a*]pyridine-8-carbonitrile (11). To a solution of **32** (0.3 g, 1.02 mmol) in dry CH₂Cl₂ (2 mL) cooled at 0 °C were added Et₃N (0.14 mL, 1.02 mmol) and 2,2-dimethylpropionyl chloride (0.15 g, 1.23 mmol). The resulting reaction mixture was gradually warmed to room temperature and further stirred for 16 h. NaHCO₃ (aqueous saturated solution) was added, and the resulting solution was then extracted with CH₂Cl₂. The organic layer was separated, dried over MgSO₄, and concentrated in vacuo. The residue thus obtained was dissolved in 1,2-dichloroethane (2 mL), and POCl₃ (0.094 mL, 1.01 mmol) was added. The resulting mixture was heated at 150 °C for 5 min under microwave irradiation. After cooling to room temperature, the mixture was diluted with CH₂Cl₂ and washed with NaHCO₃ (aqueous saturated solution). The organic layer was separated, dried over Na₂SO₄, and concentrated in vacuo. The residue thus obtained was purified by column chromatography (silica gel, EtAcO in CH₂Cl₂, 0/100 to 20/80) to give **11** (0.11 g, 31%) as a solid. Mp > 300 °C. ¹H NMR (400 MHz, CDCl₃) δ 1.55 (s, 9 H), 1.90 (qd, *J* = 12.3, 3.5 Hz, 2 H), 2.06 (dd, *J* = 12.7, 1.8 Hz, 2 H), 2.84 (tt, *J* = 12.1, 3.7 Hz, 1 H), 3.37 (td, *J* = 12.8, 2.3 Hz, 2 H), 4.31 (dt, *J* = 13.6, 2.1 Hz, 2 H), 6.57 (d, *J* = 7.9 Hz, 1 H), 7.20–7.28 (m, 3 H), 7.29–7.38 (m, 2 H), 8.05 (d, *J* = 8.1 Hz, 1 H). LCMS: *m/z* 360 [M + H]⁺, *t_R* = 3.18 min.

3-Methoxymethyl-7-(4-phenyl-1-piperidin-1-yl)-1,2,4-triazolo[4,3-*a*]pyridine-8-carbonitrile (12). To a solution of **32** (0.2 g, 0.68 mmol) in dry CH₂Cl₂ (2 mL) cooled at 0 °C were added Et₃N (0.19 mL, 1.36 mmol) and methoxyacetyl chloride (0.074 g, 0.68 mmol). The resulting reaction mixture was gradually warmed to room temperature and further stirred for 1 h. NaHCO₃ (aqueous saturated solution) was added, and the resulting solution was then extracted with CH₂Cl₂. The organic layer was separated, dried over MgSO₄, and concentrated in vacuo. The residue thus obtained was dissolved in 1,2-dichloroethane (2 mL), and POCl₃ (0.035 mL, 0.37 mmol) was added. The resulting mixture was heated at 150 °C for 5 min under microwave irradiation. After cooling to room temperature, the mixture was diluted with CH₂Cl₂ and washed with NaHCO₃ (aqueous saturated solution). The organic layer was separated, dried over Na₂SO₄, and concentrated in vacuo. The residue thus obtained was purified by column chromatography (silica gel, MeOH–NH₃ in CH₂Cl₂, 0/100 to 10/90) to give **12** (0.075 g, 32%). ¹H NMR (500 MHz, CDCl₃) δ 1.78 (qd, *J* = 12.6, 3.6 Hz, 2 H), 1.95 (br d, *J* = 11.0 Hz, 2 H), 2.92 (tt, *J* = 12.0, 3.5 Hz, 1 H), 3.29 (s, 3 H), 3.39–3.47 (m, 2 H), 4.35 (br d, *J* = 13.3 Hz, 2 H), 4.86 (s, 2 H), 7.03 (d, *J* = 7.8 Hz, 1 H), 7.19–7.25 (m, 1 H), 7.26–7.36 (m, 4 H), 8.33 (d, *J* = 8.1 Hz, 1 H). LCMS: *m/z* 348 [M + H]⁺, *t_R* = 3.62 min.

7-(4-Phenylpiperidin-1-yl)-3-pyrrolidin-1-ylmethyl[1,2,4]triazolo[4,3-*a*]pyridine-8-carbonitrile (13). To a solution of **33** (0.15 g, 0.49 mmol) in acetic acid (2 mL) were added pyrrolidine (0.63 g, 0.89 mmol) and paraformaldehyde (0.46 mL, 2.03 mmol). The resulting mixture was stirred at 80 °C for 16 h. After the mixture was cooled to room temperature, water was added. The resulting aqueous solution was extracted with CH₂Cl₂. The organic layer was separated, dried over MgSO₄, and the volatiles were evaporated in vacuo. The residue thus obtained was purified by column chromatography (silica gel, MeOH in CH₂Cl₂, 0/100 to 3/97) to give **13** as a white solid (0.084 g, 44%). ¹H NMR (400 MHz, DMSO-*d*₆) δ 1.68 (quin, *J* = 3.1 Hz, 4 H), 1.77 (qd, *J* = 12.6, 3.8 Hz, 2 H), 1.94 (dd, *J* = 12.5, 1.8 Hz, 2 H), 2.46 (br s, 4 H), 2.91 (tt, *J* = 12.0, 3.6 Hz, 1 H), 3.37–3.46 (m, 2 H), 4.04 (s, 2 H), 4.32 (br d, *J* = 13.4 Hz, 2 H), 6.98 (d, *J* = 7.9 Hz, 1 H), 7.19–7.24 (m, 1 H), 7.25–7.36 (m, 4 H), 8.36 (d, *J* = 8.1 Hz, 1 H). LCMS: *m/z* 387 [M + H]⁺, *t_R* = 4.09 min.

8-Chloro-7-(4-phenylpiperidin-1-yl)-3-(2,2,2-trifluoroethyl)-1,2,4-triazolo[4,3-*a*]pyridine (14). To a solution of **37a** (0.45 g,

1.47 mmol) in dry CH_2Cl_2 (2 mL) were added Et_3N (0.31 mL, 2.23 mmol), 3,3,3-trifluoropropionyl chloride (0.22 mL, 1.78 mmol), and the resulting mixture was stirred at room temperature for 1 h. Then the volatiles were evaporated in vacuo. The residue thus obtained was dissolved in 1,2-dichloroethane (5 mL), and POCl_3 (0.13 mL, 1.45 mmol) was added at room temperature. The resulting mixture was heated at 150 °C for 5 min under microwave irradiation. After cooling to room temperature, the mixture was diluted with CH_2Cl_2 and washed with NaHCO_3 (aqueous saturated solution). The organic layer was separated, dried over Na_2SO_4 , and concentrated in vacuo. The residue thus obtained was purified by column chromatography (silica gel EtOAc in CH_2Cl_2 , 0/100 to 10/90) to give **14** as a white solid (0.15 g, 26%). Mp 228.6 °C. $^1\text{H NMR}$ (500 MHz, CDCl_3) δ 1.94–2.06 (m, 4 H), 2.66–2.78 (m, 1 H), 3.00–3.11 (m, 2 H), 3.77 (br d, $J = 12.1$ Hz, 2 H), 4.02 (q, $J = 9.8$ Hz, 2 H), 6.85 (d, $J = 7.2$ Hz, 1 H), 7.21–7.31 (m, 3 H), 7.31–7.38 (m, 2 H), 7.86 (d, $J = 7.5$ Hz, 1 H). LCMS: m/z 395 $[\text{M} + \text{H}]^+$, $t_R = 3.66$ min.

8-Chloro-3-cyclopropylmethyl-7-(4-phenylpiperidin-1-yl)-[1,2,4]triazolo[4,3-a]pyridine (15). To a solution of **37a** (0.15 g, 0.49 mmol) in dry CH_2Cl_2 (4 mL) were added Et_3N (0.12 mL, 0.89 mmol) and cyclopropylacetyl chloride (0.059 mL, 0.49 mmol). The resulting mixture was stirred at room temperature for 1 h. Then the volatiles were evaporated in vacuo. The residue thus obtained was dissolved in 1,2-dichloroethane (5 mL), and POCl_3 (0.13 mL, 1.45 mmol) was added. The reaction mixture was heated at 150 °C for 5 min under microwave irradiation. After cooling to room temperature, the mixture was diluted with CH_2Cl_2 and washed with NaHCO_3 (aqueous saturated solution). The organic layer was separated, dried over Na_2SO_4 , and concentrated in vacuo. The residue thus obtained was purified by column chromatography (silica gel, CH_2Cl_2) to give **15** as a white solid (0.069 g, 36%). Mp 194.1 °C. $^1\text{H NMR}$ (500 MHz, CDCl_3) δ 0.26–0.39 (m, 2 H), 0.55–0.68 (m, 2 H), 1.10–1.23 (m, 1 H), 1.93–2.07 (m, 4 H), 2.65–2.77 (m, 1 H), 2.95–3.04 (m, 2 H), 3.05 (d, $J = 6.7$ Hz, 2 H), 3.72 (br d, $J = 12.0$ Hz, 2 H), 6.77 (d, $J = 7.4$ Hz, 1 H), 7.20–7.32 (m, 3 H), 7.32–7.39 (m, 2 H), 7.84 (d, $J = 7.4$ Hz, 1 H). LCMS: m/z 367 $[\text{M} + \text{H}]^+$, $t_R = 3.69$ min.

8-Chloro-3-ethyl-7-(4-phenylpiperidin-1-yl)-[1,2,4]triazolo[4,3-a]pyridine (16). A solution of **37a** (0.1 g, 0.33 mmol) and $\text{Et}(\text{OEt})_3$ (0.058 mL, 0.33 mmol) in xylene (2 mL) was heated in a sealed tube at 180 °C for 2 h. After the mixture was cooled to room temperature, the volatiles were evaporated in vacuo. The residue thus obtained was purified by column chromatography (silica gel, $\text{MeOH}-\text{NH}_3$ in CH_2Cl_2 , 0/100 to 3/97) to give **16** as a white solid (0.056 g, 50%). Mp 227.7 °C. $^1\text{H NMR}$ (500 MHz, $\text{DMSO}-d_6$) δ 1.34 (t, $J = 7.5$ Hz, 3 H), 1.84 (qd, $J = 12.1$, 3.8 Hz, 2 H), 1.91 (br d, $J = 10.4$ Hz, 2 H), 2.73 (tt, $J = 11.9$, 3.8 Hz, 1 H), 2.98–3.09 (m, 4 H), 3.62 (br d, $J = 12.1$ Hz, 2 H), 6.98 (d, $J = 7.5$ Hz, 1 H), 7.19–7.26 (m, 1 H), 7.28–7.37 (m, 4 H), 8.32 (d, $J = 7.2$ Hz, 1 H). LCMS: m/z 341 $[\text{M} + \text{H}]^+$, $t_R = 4.34$ min.

8-Chloro-7-(4-fluoro-4-phenylpiperidin-1-yl)-3-(2,2,2-trifluoroethyl)-1,2,4-triazolo[4,3-a]pyridine (17). To a solution of **37b** (6 g, 18.7 mmol) in dry CH_2Cl_2 (30 mL) cooled at 0 °C were added Et_3N (4.69 mL, 33.67 mmol) and 3,3,3-trifluoropropionyl chloride (3.08 mL, 29.93 mmol). The reaction mixture was allowed to warm to room temperature and then further stirred for 1 h. Then NaHCO_3 (aqueous saturated solution) was added, and the resulting solution was then extracted with CH_2Cl_2 . The organic layer was separated, dried over MgSO_4 , and concentrated in vacuo. The residue thus obtained was dissolved in 1,2-dichloroethane (180 mL), and polymer supported diisopropylethylamine (13.87 g, 54.09 mmol, loading 3.9 mmol/g), polymer supported PPh_3 (25.04 g, 45.07 mmol, loading 1.8 mmol/g) and trichloroacetonitrile (2.17 mL, 21.64 mmol) were added. The resulting mixture was heated at 150 °C for 10 min under microwave irradiation. After cooling to room temperature, the mixture was filtered through a Celite pad and the solids were washed thoroughly with CH_2Cl_2 and MeOH . The combined filtrates were concentrated in vacuo, and the residue thus obtained was purified by column chromatography (silica gel, EtOAc in CH_2Cl_2 , 0/100 to 40/60). The desired fractions were collected, and the volatiles were evaporated in vacuo. The resulting residue was purified by preparative

supercritical fluid purification (pyridine 20 mm; mobile phase, isocratic 83% CO_2 , 17% MeOH) to give **17** as a white solid (2.36 g, 31%). Mp > 300 °C. $^1\text{H NMR}$ (500 MHz, CDCl_3) δ 2.11–2.22 (m, 2 H), 2.30 (td, $J = 13.2$, 4.8 Hz, 1 H), 2.41 (td, $J = 13.3$, 4.9 Hz, 1 H), 3.39 (td, $J = 12.2$, 2.0 Hz, 2 H), 3.53–3.64 (m, 2 H), 4.04 (q, $J = 9.9$ Hz, 2 H), 6.90 (d, $J = 7.3$ Hz, 1 H), 7.31–7.38 (m, 1 H), 7.38–7.50 (m, 4 H), 7.91 (d, $J = 7.7$ Hz, 1 H). LCMS: m/z 413 $[\text{M} + \text{H}]^+$, $t_R = 1.05$ min.

8-Chloro-3-cyclopropylmethyl-7-(4-phenyl-4-trifluoromethylpiperidin-1-yl)-[1,2,4]triazolo[4,3-a]pyridine (18). To a stirred solution of **40** (1 g, 3 mmol) in toluene (10 mL) were added 4-trifluoromethyl-4-phenylpiperidine **41** (0.962 mL, 4.2 mmol), $\text{Pd}(\text{OAc})_2$ (0.034 g, 0.15 mmol), Cs_2CO_3 (1.46 g, 4.5 mmol), and BINAP (0.14 g, 0.225 mmol), and the reaction mixture was heated at 95 °C for 16 h in a sealed tube. After cooling to room temperature, the mixture was concentrated in vacuo and the resulting residue was suspended in water and extracted with CH_2Cl_2 . The organic layer was separated, dried (Na_2SO_4), concentrated in vacuo, and purified by column chromatography (silica gel, MeOH in CH_2Cl_2 , 0/100 to 10/90) to give **18** as a solid (0.5 g, 39%). Mp 276.7 °C. $^1\text{H NMR}$ (500 MHz, CDCl_3) δ 0.24–0.34 (m, 2 H), 0.53–0.64 (m, 2 H), 1.07–1.19 (m, 1 H), 2.38–2.48 (m, 2 H), 2.64 (d, $J = 12.7$ Hz, 2 H), 2.91 (t, $J = 11.8$ Hz, 2 H), 3.02 (d, $J = 6.6$ Hz, 2 H), 3.51 (br d, $J = 12.1$ Hz, 2 H), 6.57 (d, $J = 7.5$ Hz, 1 H), 7.36–7.42 (m, 1 H), 7.46 (t, $J = 7.7$ Hz, 2 H), 7.49–7.53 (m, 2 H), 7.76 (d, $J = 7.2$ Hz, 1 H). LCMS: m/z 435 $[\text{M} + \text{H}]^+$, $t_R = 2.43$ min.

8-Chloro-3-cyclopropylmethyl-7-(4-phenylpiperazin-1-yl)-1,2,4-triazolo[4,3-a]pyridine (19). To a stirred solution of **40** (0.3 g, 0.9 mmol) in toluene (4 mL) were added 4-phenylpiperazine **42** (0.18 mL, 1.69 mmol), $\text{Pd}(\text{OAc})_2$ (0.010 g, 0.045 mmol), Cs_2CO_3 (0.73 g, 2.24 mmol), and BINAP (0.042 g, 0.068 mmol), and the reaction mixture was heated at 95 °C for 16 h in a sealed tube. After cooling to room temperature, the mixture was concentrated in vacuo and the resulting residue was suspended in water and extracted with CH_2Cl_2 . The organic layer was separated, dried (Na_2SO_4), concentrated in vacuo, and purified by column chromatography (silica gel, EtOAc in CH_2Cl_2 , 0/100 to 40/60). The desired fractions were collected, and the volatiles were evaporated in vacuo. The residue thus obtained was precipitated by treatment with diisopropyl ether to give compound **19** as a solid (0.2 g, 60%). Mp > 300 °C. $^1\text{H NMR}$ (400 MHz, CDCl_3) δ 0.27–0.39 (m, 2 H), 0.55–0.69 (m, 2 H), 1.12–1.22 (m, 1 H), 3.06 (d, $J = 6.7$ Hz, 2 H), 3.33–3.48 (m, 8 H), 6.77 (d, $J = 7.4$ Hz, 1 H), 6.92 (t, $J = 7.3$ Hz, 1 H), 7.00 (d, $J = 8.1$ Hz, 2 H), 7.31 (t, $J = 8.1$ Hz, 2 H), 7.88 (d, $J = 7.4$ Hz, 1 H). LCMS: m/z 368 $[\text{M} + \text{H}]^+$, $t_R = 2.79$ min.

3-Cyclopropylmethyl-7-(4-phenylpiperidin-1-yl)-8-trifluoromethyl-1,2,4-triazolo[4,3-a]pyridine (20). A mixture of **46** (4 g, 14.51 mmol), 4-phenylpiperidine **30** (3.3 g, 17.41 mmol), and diisopropylethylamine (5.05 mL, 29.02 mmol) in CH_3CN (8.5 mL) was heated at 180 °C for 20 min under microwave irradiation. After cooling to room temperature, the mixture was concentrated in vacuo. The residue thus obtained was purified by column chromatography (silica gel, $\text{MeOH}-\text{NH}_3$ in CH_2Cl_2 , 0/100 to 10/90) to give **20** as a solid (2.8 g, 48%). Mp 211.3 °C. $^1\text{H NMR}$ (500 MHz, CDCl_3) δ 0.28–0.39 (m, 2 H), 0.57–0.72 (m, 2 H), 1.06–1.22 (m, 1 H), 1.78–2.11 (m, 4 H), 2.72 (tt, $J = 11.5$, 4.4 Hz, 1 H), 3.04 (d, $J = 6.6$ Hz, 2 H), 3.18 (td, $J = 12.1$, 2.0 Hz, 2 H), 3.62 (br d, $J = 12.4$ Hz, 2 H), 6.76 (d, $J = 7.5$ Hz, 1 H), 7.21–7.28 (m, 3 H), 7.34 (t, $J = 7.7$ Hz, 2 H), 7.92 (d, $J = 7.8$ Hz, 1 H). LCMS: m/z 401 $[\text{M} + \text{H}]^+$, $t_R = 4.78$ min.

3-Ethyl-7-(4-phenylpiperidin-1-yl)-8-trifluoromethyl-1,2,4-triazolo[4,3-a]pyridine (21). To a solution of **50a** (2.6 g, 7.73 mmol) in dry CH_2Cl_2 (70 mL) at 0 °C were added Et_3N (1.9 mL, 13.91 mmol) and propanoyl chloride (0.83 mL, 9.28 mmol). The resulting reaction mixture was stirred at room temperature for 10 min. The mixture was then concentrated in vacuo. The residue thus obtained was dissolved in 1,2-dichloroethane (5 mL), and POCl_3 (0.7 mL, 1.15 mmol) was added. The resulting mixture was heated at 150 °C for 5 min under microwave irradiation. After cooling to room temperature, the mixture was diluted with CH_2Cl_2 and washed with NaHCO_3 (aqueous saturated solution). The organic layer was separated, dried over Na_2SO_4 , and concentrated in vacuo. The crude

product was purified by column chromatography (silica gel, CH₂Cl₂) to give **21** (0.14 g, 50%). ¹H NMR (500 MHz, CDCl₃) δ 1.46 (t, *J* = 7.5 Hz, 3 H), 1.87–2.01 (m, 4 H), 2.72 (tt, *J* = 11.5, 4.3 Hz, 1 H), 3.06 (q, *J* = 7.5 Hz, 2 H), 3.18 (td, *J* = 12.4, 2.3 Hz, 2 H), 3.62 (br d, *J* = 12.7 Hz, 2 H), 6.77 (d, *J* = 7.5 Hz, 1 H), 7.21–7.28 (m, 3 H), 7.31–7.37 (m, 2 H), 7.81 (d, *J* = 7.5 Hz, 1 H). LCMS: *m/z* 375 [M + H]⁺, *t_R* = 4.4 min.

3-Butyl-7-(4-phenylpiperidin-1-yl)-8-trifluoromethyl-1,2,4-triazolo[4,3-*a*]pyridine (22). To a solution of **50a** (0.35 g, 1.04 mmol) in dry CH₂Cl₂ (10 mL) was added Et₃N (0.25 mL, 1.87 mmol) and pentanoyl chloride (0.13 mL, 1.04 mmol). The resulting reaction mixture was stirred at room temperature for 10 min. The mixture was then concentrated in vacuo. The residue thus obtained was dissolved in 1,2-dichloroethane (5 mL), and POCl₃ (0.15 mL, 1.57 mmol) was added. The resulting mixture was heated at 150 °C for 5 min under microwave irradiation. After cooling to room temperature, the mixture was diluted with CH₂Cl₂ and washed with NaHCO₃ (aqueous saturated solution). The organic layer was separated, dried over Na₂SO₄, and concentrated in vacuo. The residue thus obtained was purified by column chromatography (silica gel, MeOH–NH₃ in CH₂Cl₂, 0/100 to 3/97) to give **22** as a solid (0.16 g, 38%). Mp 221.7 °C. ¹H NMR (500 MHz, CDCl₃) δ 0.97 (t, *J* = 7.3 Hz, 3 H), 1.42–1.53 (m, 2 H), 1.78–1.87 (m, 2 H), 1.87–2.02 (m, 4 H), 2.65–2.78 (m, 1 H), 2.99–3.08 (m, 2 H), 3.12–3.24 (m, 2 H), 3.61 (br d, *J* = 12.5 Hz, 2 H), 6.76 (d, *J* = 7.6 Hz, 1 H), 7.20–7.30 (m, 3 H), 7.30–7.39 (m, 2 H), 7.81 (d, *J* = 7.9 Hz, 1 H). LCMS: *m/z* 403 [M + H]⁺, *t_R* = 3.96 min.

3-Cyclopropylmethyl-7-(4-fluoro-4-phenylpiperidin-1-yl)-8-trifluoromethyl-1,2,4-triazolo[4,3-*a*]pyridine (23). To a solution of **50b** (0.29 g, 0.82 mmol) in dry CH₂Cl₂ (10 mL) were added Et₃N (0.2 mL, 1.47 mmol) and cyclopropylacetyl chloride (0.12 g, 0.98 mmol). The resulting reaction mixture was stirred at room temperature for 10 min. The mixture was then concentrated in vacuo. The residue was dissolved in 1,2-dichloroethane (10 mL), and polymer supported diisopropylethylamine (0.65 g, 2.54 mmol, loading 3.9 mmol/g), polymer supported PPh₃ (1.77 g, 2.12 mmol, loading 1.8 mmol/g), and trichloroacetonitrile (0.1 mL, 1.02 mmol) were added. The resulting mixture was heated at 150 °C for 10 min under microwave irradiation. After cooling to room temperature, the mixture was filtered through a Celite pad and the solids were washed thoroughly with CH₂Cl₂ and MeOH. The combined filtrates were concentrated in vacuo and the residue thus obtained was purified by column chromatography (silica gel, EtOAc in CH₂Cl₂, 0/100 to 40/60) to give a residue that was purified by supercritical fluid purification (pyridine 20 mm; mobile phase, isocratic 85% CO₂, 15% MeOH) to give **23** as a solid (0.1 g, 29%). ¹H NMR (500 MHz, CDCl₃) δ 0.27–0.41 (m, 2 H), 0.57–0.70 (m, 2 H), 1.11–1.22 (m, 1 H), 2.08–2.19 (m, 2 H), 2.20–2.31 (m, 1 H), 2.36 (td, *J* = 13.2, 5.1 Hz, 1 H), 3.06 (d, *J* = 6.5 Hz, 2 H), 3.33–3.43 (m, 2 H), 3.43–3.55 (m, 2 H), 6.83 (d, *J* = 7.6 Hz, 1 H), 7.31–7.37 (m, 1 H), 7.38–7.48 (m, 4 H), 7.98 (d, *J* = 7.6 Hz, 1 H). LCMS: *m/z* 419 [M + H]⁺, *t_R* = 1.09 min.

2-(3-Cyclopropylmethyl-8-trifluoromethyl[1,2,4]triazolo[4,3-*a*]pyridin-7-yl)-1,2,3,4-tetrahydroisoquinoline (24). A mixture of **46** (0.25 g, 0.91 mmol), 1,2,3,4-tetrahydroisoquinoline (0.14 mL, 1.09 mmol), and diisopropylethylamine (0.31 mL, 1.81 mmol) in CH₃CN (5 mL) was heated at 180 °C for 20 min under microwave irradiation. After cooling to room temperature, the mixture was concentrated in vacuo. The crude product was purified by column chromatography (silica gel, MeOH–NH₃ in CH₂Cl₂, 0/100 to 1/99) to give **24** as a solid (0.12 g, 36%). Mp > 300 °C. ¹H NMR (400 MHz, CDCl₃) δ 0.26–0.38 (m, 2 H), 0.54–0.67 (m, 2 H), 1.07–1.17 (m, 1 H), 2.99–3.05 (m, 2 H), 3.03 (d, *J* = 6.7 Hz, 2 H), 3.68 (t, *J* = 5.9 Hz, 2 H), 4.52 (s, 2 H), 6.79 (d, *J* = 7.9 Hz, 1 H), 7.08–7.14 (m, 1 H), 7.14–7.25 (m, 3 H), 7.89 (d, *J* = 7.6 Hz, 1 H). LCMS: *m/z* 373 [M + H]⁺, *t_R* = 4.2 min.

3-Cyclopropylmethyl-7-(1,3-dihydroisoindol-2-yl)-8-trifluoromethyl[1,2,4]triazolo[4,3-*a*]pyridine (25). A mixture of **46** (0.2 g, 0.73 mmol), isoindoline (0.17 g, 1.45 mmol), and diisopropylethylamine (0.76 mL, 4.35 mmol) in CH₃CN (10 mL) was heated at 180 °C for 20 min under microwave irradiation. After

cooling to room temperature, the mixture was concentrated in vacuo. The crude product was purified by column chromatography (silica gel, MeOH–NH₃ in CH₂Cl₂, 0/100 to 1/99) to give **25** as a solid (0.13 g, 50%). Mp > 300 °C. ¹H NMR (500 MHz, CDCl₃) δ 0.28–0.37 (m, 2 H), 0.56–0.66 (m, 2 H), 1.10–1.18 (m, 1 H), 3.02 (d, *J* = 6.6 Hz, 2 H), 5.00 (s, 4 H), 6.80 (d, *J* = 7.8 Hz, 1 H), 7.30–7.37 (m, 4 H), 7.85 (d, *J* = 7.8 Hz, 1 H). LCMS: *m/z* 359 [M + H]⁺, *t_R* = 2.66 min.

rac-3-Cyclopropylmethyl-7-(3-phenylpyrrolidin-1-yl)-8-trifluoromethyl[1,2,4]triazolo[4,3-*a*]pyridine (26). A mixture of **46** (0.2 g, 0.73 mmol), *rac*-3-phenylpyrrolidine (0.21 g, 1.45 mmol), and diisopropylethylamine (0.76 mL, 4.35 mmol) in CH₃CN (10 mL) was heated at 180 °C for 20 min under microwave irradiation. After cooling, the mixture was concentrated in vacuo. The crude product was purified by column chromatography (silica gel, MeOH–NH₃ in CH₂Cl₂, 0/100 to 1/99) to give **26** as a solid (0.092 g, 32%). Mp 178.3 °C. ¹H NMR (500 MHz, CDCl₃) δ 0.26–0.37 (m, 2 H), 0.56–0.64 (m, 2 H), 1.08–1.18 (m, 1 H), 2.10–2.21 (m, 1 H), 2.36–2.45 (m, 1 H), 2.94–3.06 (m, 2 H), 3.44–3.53 (m, 1 H), 3.65–3.73 (m, 2 H), 3.76–3.84 (m, 1 H), 3.84–3.91 (m, 1 H), 6.68 (d, *J* = 7.8 Hz, 1 H), 7.23–7.32 (m, 3 H), 7.33–7.39 (m, 2 H), 7.79 (d, *J* = 7.8 Hz, 1 H). LCMS: *m/z* 387 [M + H]⁺, *t_R* = 2.18 min.

3-Cyclopropylmethyl-7-[4-(2,4-difluorophenyl)piperidin-1-yl]-8-trifluoromethyl[1,2,4]triazolo[4,3-*a*]pyridine (27). A mixture of **46** (0.06 g, 0.22 mmol), 4-(2,4-difluorophenyl)piperidine **27** (0.061 g, 0.261 mmol), and diisopropylethylamine (0.076 mL, 0.43 mmol) in CH₃CN (2 mL) was heated at 180 °C for 15 min under microwave irradiation. After the mixture was cooled to room temperature, the volatiles were evaporated in vacuo. The residue thus obtained was purified by column chromatography (silica gel, EtOAc in CH₂Cl₂, 0/100 to 30/70) to give **27** as a solid (0.041 g, 43%). Mp > 300 °C. ¹H NMR (500 MHz, CDCl₃) δ 0.28–0.39 (m, 2 H), 0.57–0.68 (m, 2 H), 1.11–1.19 (m, 1 H), 1.86–1.97 (m, 4 H), 2.97–3.08 (m, 1 H), 3.05 (d, *J* = 6.6 Hz, 2 H), 3.13–3.24 (m, 2 H), 3.60 (d, *J* = 12.1 Hz, 2 H), 6.77 (d, *J* = 7.5 Hz, 1 H), 6.81 (ddd, *J* = 10.7, 8.7, 2.6 Hz, 1 H), 6.87 (td, *J* = 8.3, 2.2 Hz, 1 H), 7.22 (td, *J* = 8.5, 6.6 Hz, 1 H), 7.94 (d, *J* = 7.5 Hz, 1 H). LCMS: *m/z* 437 [M + H]⁺, *t_R* = 2.55 min.

1'-(3-Cyclopropylmethyl-8-trifluoromethyl[1,2,4]triazolo[4,3-*a*]pyridin-7-yl)-1',2',3',4',5',6'-hexahydro[3,4']bipyridinyl (28). A mixture of **46** (0.22 g, 0.8 mmol), 4-(3-pyridyl)piperidine (0.14 g, 0.84 mmol), and diisopropylethylamine (0.17 mL, 0.96 mmol) in CH₃CN (5 mL) was heated at 90 °C for 1 day. After the mixture was cooled to room temperature, the volatiles were evaporated in vacuo. The residue thus obtained was purified by column chromatography (silica gel, EtOAc in CH₂Cl₂, 0/100 to 30/70) to give **28** as a solid (0.11 g, 35%). Mp 201.9 °C. ¹H NMR (400 MHz, CDCl₃) δ 0.27–0.40 (m, 2 H), 0.55–0.69 (m, 2 H), 1.09–1.22 (m, 1 H), 1.86–2.03 (m, 4 H), 2.70–2.81 (m, 1 H), 3.05 (d, *J* = 6.7 Hz, 2 H), 3.12–3.24 (m, 2 H), 3.61 (br d, *J* = 12.5 Hz, 2 H), 6.77 (d, *J* = 7.6 Hz, 1 H), 7.28 (dd, *J* = 8.1, 4.9 Hz, 1 H), 7.58 (dt, *J* = 8.0, 1.9 Hz, 1 H), 7.95 (d, *J* = 7.6 Hz, 1 H), 8.50 (dd, *J* = 4.7, 1.5 Hz, 1 H), 8.54 (d, *J* = 2.1 Hz, 1 H). LCMS: *m/z* 402 [M + H]⁺, *t_R* = 1.58 min.

2-Bromo-3-cyano-4-(4-phenylpiperidin-1-yl)pyridine (31). To a suspension of NaH (0.15 g, 3.82 mmol, 60% in mineral oil) in DMF (20 mL) at 0 °C was added portionwise 4-phenylpiperidine **30** (0.62 g, 3.82 mmol). The resulting mixture was stirred at 0 °C for 5 min, and then 2,4-dibromo-3-cyanopyridine **29** (1 g, 3.016 mmol) was added. The resulting reaction mixture was stirred for 1 h. The reaction mixture was then quenched with NH₄Cl (aqueous saturated solution) and extracted with Et₂O. The organic layer was separated, dried over Na₂SO₄, and the volatiles were evaporated in vacuo. The residue thus obtained was purified by column chromatography (silica gel, MeOH–NH₃ in CH₂Cl₂, 0/100 to 1/99) to give **31** (0.98 g, 75%). ¹H NMR (500 MHz, CDCl₃) δ 1.91 (qd, *J* = 12.7, 3.6 Hz, 2 H), 2.03 (br d, *J* = 12.4 Hz, 2 H), 2.80 (tt, *J* = 12.1, 3.6 Hz, 1 H), 3.19 (br t, *J* = 12.1 Hz, 2 H), 4.15 (br d, *J* = 13.0 Hz, 2 H), 6.76 (d, *J* = 6.1 Hz, 1 H), 7.21–7.28 (m, 3 H), 7.30–7.37 (m, 2 H), 8.10 (d, *J* = 6.1 Hz, 1 H). LCMS: *m/z* 342 [M + H]⁺, *t_R* = 4.48 min.

[3-Cyano-4-(4-phenylpiperidin-1-yl)pyridin-2-yl]hydrazine (32). To a solution of **31** (0.5 g, 1.46 mmol) in THF (4 mL) at room

temperature was added hydrazine monohydrate (0.37 g, 7.30 mmol), and the mixture was heated at 160 °C for 15 min under microwave irradiation. The reaction mixture was then cooled to room temperature, and the volatiles were evaporated in vacuo. The residue thus obtained was purified by column chromatography (silica gel, MeOH–NH₃ in CH₂Cl₂, 0/100 to 1/99) to give **32** as a white solid (0.38 g, 89%). ¹H NMR (400 MHz, DMSO-*d*₆) δ 1.71 (qd, *J* = 12.6, 3.7 Hz, 2 H), 1.88 (dd, *J* = 12.0, 1.4 Hz, 2 H), 2.78 (tt, *J* = 12.0, 3.7 Hz, 1 H), 3.07 (td, *J* = 12.5, 2.1 Hz, 2 H), 3.97 (br d, *J* = 12.9 Hz, 2 H), 4.28 (s, 2 H), 6.34 (d, *J* = 6.2 Hz, 1 H), 7.17–7.24 (m, 1 H), 7.24–7.35 (m, 4 H), 7.77 (s, 1 H), 7.96 (d, *J* = 6.0 Hz, 1 H). LCMS: *m/z* 294 [M + H]⁺, *t*_R = 3.62 min.

7-(4-Phenylpiperidin-1-yl)[1,2,4]triazolo[4,3-*a*]pyridine-8-carbonitrile (33). A mixture of **32** (1 g, 3.41 mmol) and HC(OEt)₃ (7.58 g, 51.13 mmol) in xylenes (25 mL) was heated in a sealed tube at 180 °C for 2 h. The reaction mixture was cooled to room temperature and then concentrated in vacuo. The residue thus obtained was treated with Et₂O and the resulting solid was filtered off and dried in the vacuum oven (50 °C) to give **33** (0.93 g, 90%). ¹H NMR (400 MHz, DMSO-*d*₆) δ 1.77 (qd, *J* = 12.6, 3.6 Hz, 2 H), 1.89–1.99 (m, 2 H), 2.91 (tt, *J* = 12.1, 3.7 Hz, 1 H), 3.25–3.45 (m, 2 H), 4.32 (br d, *J* = 13.4 Hz, 2 H), 7.00 (d, *J* = 7.9 Hz, 1 H), 7.19–7.25 (m, 1 H), 7.25–7.36 (m, 4 H), 8.45 (d, *J* = 7.9 Hz, 1 H), 8.98 (s, 1 H). LCMS: *m/z* 304 [M + H]⁺, *t*_R = 3.11 min.

2',3'-Dichloro-4-phenyl-3,4,5,6-tetrahydro-2H-[1,4']-bipyridinyl (36a). A mixture of 2,3-dichloro-4-iodopyridine **34** (4 g, 14.61 mmol), 4-phenylpiperidine **30** (3.53 g, 21.91 mmol), and diisopropylethylamine (5.09 mL, 29.21 mmol) in CH₃CN (150 mL) was heated in a sealed tube at 110 °C for 16 h. The mixture was then cooled to room temperature, and then NaHCO₃ (aqueous saturated solution) was added. The resulting mixture was extracted with EtOAc. The organic layer was separated, dried (Na₂SO₄), and the volatiles were evaporated in vacuo. The residue thus obtained was purified by column chromatography (silica gel, MeOH–NH₃ in CH₂Cl₂, 0/100 to 1/99). The desired fractions were collected and concentrated in vacuo to give **36a** as a white solid (2.32 g, 52%). ¹H NMR (400 MHz, DMSO-*d*₆) δ 1.80 (qd, *J* = 12.3, 3.7 Hz, 2 H), 1.90 (dd, *J* = 12.3, 2.3 Hz, 2 H), 2.75 (tt, *J* = 12.0, 3.8 Hz, 1 H), 2.93 (td, *J* = 12.1, 2.1 Hz, 2 H), 3.68 (br d, *J* = 12.5 Hz, 2 H), 7.14 (d, *J* = 5.5 Hz, 1 H), 7.18–7.24 (m, 1 H), 7.26–7.35 (m, 4 H), 8.16 (d, *J* = 5.5 Hz, 1 H). LCMS: *m/z* 307 [M + H]⁺, *t*_R = 3.46 min.

2',3'-Dichloro-4-fluoro-4-phenyl-3,4,5,6-tetrahydro-2H-[1,4']bipyridinyl (36b). A mixture of 2,3-dichloro-4-iodopyridine **34** (2 g, 7.30 mmol), 4-fluoro-4-phenylpiperidine hydrochloride **35** (2.05 g, 9.49 mmol), and diisopropylethylamine (5.05 mL, 29.21 mmol) in CH₃CN (10 mL) was heated in a sealed tube at 110 °C for 16 h. The mixture was cooled to room temperature, and then NaHCO₃ (aqueous saturated solution) was added. The resulting mixture was extracted with EtOAc. The organic layer was separated, dried over Na₂SO₄, and the volatiles were evaporated in vacuo. The residue thus obtained was purified by column chromatography (silica gel, CH₂Cl₂ in heptane 25/75 to 75/25) to give **36b** as a white solid (0.88 g, 37%). ¹H NMR (500 MHz, CDCl₃) δ 2.08–2.20 (m, 2 H), 2.27 (ddd, *J* = 13.6, 13.0, 4.6 Hz, 1 H), 2.35 (td, *J* = 13.3, 4.9 Hz, 1 H), 3.25 (td, *J* = 12.3, 2.0 Hz, 2 H), 3.53–3.63 (m, 2 H), 6.90 (d, *J* = 5.5 Hz, 1 H), 7.31–7.37 (m, 1 H), 7.38–7.49 (m, 4 H), 8.14 (d, *J* = 5.5 Hz, 1 H). LCMS: *m/z* 325 [M + H]⁺, *t*_R = 3.32 min.

(3'-Chloro-4-phenyl-3,4,5,6-tetrahydro-2H-[1,4']bipyridinyl-2'-yl)hydrazine (37a). To a suspension of **36a** (0.25 g, 0.81 mmol) in 1,4-dioxane (3 mL) at room temperature was added hydrazine monohydrate (0.79 mL, 16.27 mmol). The reaction mixture was heated at 160 °C for 20 min under microwave irradiation. After the mixture was cooled to room temperature, the solvent was evaporated in vacuo, and the residue thus obtained was taken up in CH₂Cl₂. The resulting solution was washed with NaHCO₃ (aqueous saturated solution). The organic layer was separated, dried over MgSO₄, and concentrated in vacuo to give **37a** (0.24 g, 99%). ¹H NMR (400 MHz, DMSO-*d*₆) δ 1.79 (qd, *J* = 12.3, 3.7 Hz, 2 H), 1.84–1.91 (m, 2 H), 2.63–2.75 (m, 1 H), 2.81 (td, *J* = 11.8, 2.1 Hz, 2 H), 3.54 (br d, *J* = 12.0 Hz, 2 H), 4.16 (s, 2 H), 6.48 (d, *J* = 5.5 Hz, 1 H), 7.18–7.24 (m,

1 H), 7.26–7.36 (m, 5 H), 7.93 (d, *J* = 5.5 Hz, 1 H). LCMS: *m/z* 303 [M + H]⁺, *t*_R = 4.13 min.

(3'-Chloro-4-fluoro-4-phenyl-3,4,5,6-tetrahydro-2H-[1,4']-bipyridinyl-2'-yl)hydrazine (37b). To a suspension of compound **36b** (0.97 g, 2.97 mmol) in EtOH (6 mL) was added hydrazine monohydrate (2.88 mL, 59.41 mmol). The reaction mixture was heated under microwave irradiation at 160 °C for 20 min. After the mixture was cooled to room temperature, the volatiles were evaporated in vacuo and the residue thus obtained was taken up in CH₂Cl₂. The resulting solution was washed with NaHCO₃ (aqueous saturated solution). The organic layer was separated, dried over MgSO₄, and concentrated in vacuo. The residue thus obtained was precipitated by treatment with Et₂O. The resulting solid was filtered off and dried in the vacuum oven (50 °C) to give **37b** as a white solid (0.8 g, 84%). ¹H NMR (400 MHz, DMSO-*d*₆) δ 2.04 (dd, *J* = 12.3, 11.3 Hz, 2 H), 2.19 (td, *J* = 13.2, 4.6 Hz, 1 H), 2.29 (td, *J* = 13.4, 4.0 Hz, 1 H), 3.07 (t, *J* = 11.4 Hz, 2 H), 3.37–3.49 (m, 2 H), 4.17 (s, 2 H), 6.53 (d, *J* = 5.8 Hz, 1 H), 7.31–7.39 (m, 2 H), 7.42 (t, *J* = 7.5 Hz, 2 H), 7.46–7.53 (m, 2 H), 7.95 (d, *J* = 5.5 Hz, 1 H). LCMS: *m/z* 321 [M + H]⁺, *t*_R = 3.37 min.

(3-Chloro-4-iodopyridin-2-yl)hydrazine (38). To a solution of 2,3-dichloro-4-iodopyridine **34** (8 g, 29.21 mmol) in 1,4-dioxane (450 mL) was added hydrazine monohydrate (14.17 mL, 175.25 mmol). The reaction mixture was heated in a sealed tube at 70 °C for 16 h. After the mixture was cooled to room temperature, NH₄OH (32% aqueous solution) was added and the resulting mixture was concentrated in vacuo. The resulting residue was taken up in EtOH, and the suspension thus obtained was heated to reflux. The remaining solid was filtered off while hot, and the filtrate was cooled to room temperature. The precipitate newly formed was filtered off and then the filtrate concentrated in vacuo to give **38** as a white solid (2.67 g, 52%). ¹H NMR (400 MHz, DMSO-*d*₆) δ 3.90 (br s, 3 H), 7.10 (d, *J* = 5.1 Hz, 1 H), 7.70 (d, *J* = 5.1 Hz, 1 H), 7.84 (br s, 1 H). LCMS: *m/z* 270 [M + H]⁺, *t*_R = 1.13 min.

Cyclopropylacetic Acid N'-(3-Chloro-4-iodopyridin-2-yl)-hydrazide (39). To a solution of **38** (0.73 g, 2.71 mmol) in dry CH₂Cl₂ (8 mL), cooled at 0 °C, were added Et₃N (0.56 mL, 4.06 mmol) and cyclopropylacetyl chloride (0.38 g, 3.25 mmol). The reaction mixture was stirred at room temperature for 16 h, and then NaHCO₃ (aqueous saturated solution) was added. The resulting solution was extracted with CH₂Cl₂. The organic layer was separated, dried over Na₂SO₄, and concentrated in vacuo to give **39** (0.94 g, 99%). ¹H NMR (400 MHz, CDCl₃) δ 0.27–0.40 (m, 2 H), 0.56–0.70 (m, 2 H), 1.11–1.23 (m, 1 H), 1.68 (s, 2 H), 3.07 (d, *J* = 6.7 Hz, 2 H), 7.17 (d, *J* = 7.2 Hz, 1 H), 7.69 (d, *J* = 7.2 Hz, 1 H). LCMS: *m/z* 352 [M + H]⁺, *t*_R = 1.82 min.

8-Chloro-3-cyclopropylmethyl-7-iodo[1,2,4]triazolo[4,3-*a*]pyridine (40). Compound **39** (0.74 g, 2.39 mmol) was heated at 160 °C for 3 h. After the mixture was cooled to room temperature, the brown gum thus obtained was triturated with diisopropyl ether to give a solid that was filtered off and dried in the vacuum oven (50 °C), yielding **40** (0.74 g, 93%). ¹H NMR (400 MHz, CDCl₃) δ 0.26–0.41 (m, 2 H), 0.56–0.70 (m, 2 H), 1.12–1.24 (m, 1 H), 3.07 (d, *J* = 6.7 Hz, 2 H), 7.18 (d, *J* = 7.2 Hz, 1 H), 7.69 (d, *J* = 7.2 Hz, 1 H). LCMS: *m/z* 334 [M + H]⁺, *t*_R = 1.5 min.

4-Benzyloxy-2-chloro-3-trifluoromethylpyridine (44). To a suspension of NaH (0.49 g, 12.73 mmol, 60% in mineral oil) in DMF (50 mL) cooled at 0 °C was added benzyl alcohol (1.26 mL, 12.2 mmol). The resulting mixture was stirred for 2 min, and then **43** (2.5 g, 11.57 mmol) was added. The mixture was gradually warmed to room temperature and further stirred for 1 h. The reaction mixture was quenched with water and extracted with Et₂O. The organic layer was separated, dried over Na₂SO₄, and concentrated in vacuo. The residue thus obtained was purified by column chromatography (silica gel, heptane in CH₂Cl₂ 0/100 to 50/50) to give **44** (1.1 g, 33%). ¹H NMR (500 MHz, CDCl₃) δ 5.25 (s, 2 H), 6.93 (d, *J* = 5.8 Hz, 1 H), 7.33–7.39 (m, 2 H), 7.38–7.44 (m, 3 H), 8.33 (d, *J* = 5.8 Hz, 1 H). LCMS: *m/z* 288 [M + H]⁺, *t*_R = 2.57 min.

(4-Benzyloxy-3-trifluoromethylpyridin-2-yl)hydrazine (45). To a suspension of **44** (1.09 g, 3.79 mmol) in 1,4-dioxane (9 mL),

was added hydrazine monohydrate (3.68 mL, 75.78 mmol). The reaction mixture was heated at 160 °C for 30 min under microwave irradiation. After the mixture was cooled to room temperature, the volatiles were evaporated in vacuo. The residue thus obtained was dissolved in CH₂Cl₂ and washed with NaHCO₃ (aqueous saturated solution). The organic layer was separated, dried over Na₂SO₄, and concentrated in vacuo to give **45** as a white solid (0.89 g, 83%). ¹H NMR (500 MHz, CDCl₃) δ 4.01 (br s, 2 H), 5.18 (s, 2 H), 6.39 (d, *J* = 5.8 Hz, 1 H), 6.53 (br s, 1 H), 7.31–7.41 (m, 3 H), 7.39 (d, *J* = 4.6 Hz, 2 H), 8.15 (d, *J* = 5.8 Hz, 1 H). LCMS: *m/z* 284 [M + H]⁺, *t_R* = 1.88 min.

7-Chloro-3-cyclopropylmethyl-8-trifluoromethyl[1,2,4]-triazolo[4,3-*a*]pyridine (46). A mixture of **45** (1.14 g, 1.87 mmol) and POCl₃ (0.35 mL, 3.74 mmol) in 1,2-dichloroethane (10 mL) was heated at 150 °C under microwave irradiation for 10 min. After cooling to room temperature, the resulting reaction mixture was diluted with CH₂Cl₂ and washed with NaHCO₃ (aqueous saturated solution). The organic layer was separated, dried over Na₂SO₄, and the volatiles were evaporated in vacuo. The residue thus obtained was purified by column chromatography (silica gel, MeOH–NH₃ in CH₂Cl₂, 0/100 to 20/80) to give **46** as a white solid (0.26 g, 51%). Mp 184.5 °C. ¹H NMR (400 MHz, CDCl₃) δ 0.28–0.40 (m, 2 H), 0.58–0.71 (m, 2 H), 1.11–1.24 (m, 1 H), 3.10 (d, *J* = 6.7 Hz, 2 H), 6.92 (d, *J* = 7.4 Hz, 1 H), 8.05 (d, *J* = 7.4 Hz, 1 H). LCMS: *m/z* 276 [M + H]⁺, *t_R* = 1.79 min.

2'-Chloro-4-phenyl-3'-trifluoromethyl-3,4,5,6-tetrahydro-2H-[1,4']bipyridinyl (49a). To a suspension of NaH (0.19 g, 4.83 mmol, 60% in mineral oil) in DMF (20 mL) cooled at 0 °C was added 4-phenylpiperidine **30** (0.84 g, 5.24 mmol). The resulting reaction mixture was stirred at 0 °C for 10 min, and then **43** (0.87 g, 4.03 mmol) was added. The reaction mixture was allowed to warm to room temperature and further stirred for 1 h. The mixture was then quenched with water and extracted with Et₂O. The organic layer was separated, dried (Na₂SO₄), and the volatiles were evaporated in vacuo. The residue thus obtained was purified by column chromatography (silica gel, MeOH–NH₃ in CH₂Cl₂, 0/100 to 2/98) to give **49a** as a solid (0.73 g, 53%). Mp 111.4 °C. ¹H NMR (400 MHz, CDCl₃) δ 1.84–2.00 (m, 4 H), 2.63–2.75 (m, 1 H), 3.05 (td, *J* = 12.0, 3.0 Hz, 2 H), 3.58 (br d, *J* = 12.7 Hz, 2 H), 6.88 (d, *J* = 5.8 Hz, 1 H), 7.19–7.29 (m, 3 H), 7.29–7.37 (m, 2 H), 8.17 (d, *J* = 5.8 Hz, 1 H). LCMS: *m/z* 341 [M + H]⁺, *t_R* = 3.13 min.

2'-Chloro-4-fluoro-4-phenyl-3'-trifluoromethyl-3,4,5,6-tetrahydro-2H-[1,4']bipyridinyl (49b). A mixture of **43** (0.4 g, 1.85 mmol), 4-fluoro-4-phenylpiperidine hydrochloride **35** (0.4 g, 1.85 mmol), and diisopropyletamine (0.645 mL, 3.70 mmol) in CH₃CN (4 mL) was heated in a sealed tube at 110 °C for 4 h. The mixture was cooled to room temperature, diluted with EtOAc, and washed with NaHCO₃ (aqueous saturated solution). The organic layer was separated, dried over Na₂SO₄, and the volatiles were evaporated in vacuo to give a residue that was purified by column chromatography (silica gel, CH₂Cl₂) to give **49b** (0.53 g, 62%). ¹H NMR (500 MHz, CDCl₃) δ 2.08–2.17 (m, 2 H), 2.23 (dt, *J* = 14.3, 8.8 Hz, 1 H), 2.31 (dt, *J* = 13.9, 8.8 Hz, 1 H), 3.40 (br d, *J* = 8.1 Hz, 4 H), 6.94 (d, *J* = 5.8 Hz, 1 H), 7.32–7.38 (m, 1 H), 7.38–7.45 (m, 4 H), 8.23 (d, *J* = 5.5 Hz, 1 H). LCMS: *m/z* 359 [M + H]⁺, *t_R* = 3.98 min.

(4-Phenyl-3'-trifluoromethyl-3,4,5,6-tetrahydro-2H-[1,4']-bipyridinyl-2'-yl)hydrazine (50a). To a suspension of compound **49a** (0.35 g, 1.03 mmol) in THF (6 mL) at room temperature was added hydrazine monohydrate (0.2 mL, 4.11 mmol). The reaction mixture was heated at 160 °C for 45 min under microwave irradiation. Addition of hydrazine monohydrate (0.2 and 0.25 mL) to the reaction mixture followed by heating at 160 °C under microwave irradiation for 45 min was repeated twice. After cooling to room temperature, the resulting solution was concentrated in vacuo and the residue thus obtained was precipitated by treatment with Et₂O to give **50a** as a white solid (0.32 g, 93%). ¹H NMR (400 MHz, DMSO-*d*₆) δ 1.82–1.92 (m, 2 H), 1.99 (qd, *J* = 12.5, 3.9 Hz, 2 H), 2.65–2.76 (m, 1 H), 2.86 (br t, *J* = 11.2, 2 H), 3.84 (br d, *J* = 12.3 Hz, 2 H), 4.90 (s, 2 H), 6.38 (d, *J* = 5.3 Hz, 1 H), 7.16–7.25 (m, 1 H), 7.25–7.38 (m, 5 H), 8.08 (d, *J* = 5.1 Hz, 1 H). LCMS: *m/z* 337 [M + H]⁺, *t_R* = 2.94 min.

(4-Fluoro-4-phenyl-3'-trifluoromethyl-3,4,5,6-tetrahydro-2H-[1,4']bipyridinyl-2'-yl)hydrazine (50b). To a suspension of compound **49b** (0.53 g, 1.15 mmol) in THF (10 mL) was added hydrazine monohydrate (0.224 mL, 4.61 mmol). The reaction mixture was heated at 160 °C for 45 min under microwave irradiation. After the mixture was cooled to room temperature, the volatiles were evaporated in vacuo. The residue thus obtained was precipitated by treatment with Et₂O to give **50b** as a white solid (0.28 g, 69%). ¹H NMR (500 MHz, CDCl₃) δ 2.03–2.12 (m, 2 H), 2.16–2.25 (m, 1 H), 2.25–2.34 (m, 1 H), 3.22–3.32 (m, 4 H), 4.04 (br s, 2 H), 6.26 (br s, 1 H), 6.49 (d, *J* = 5.8 Hz, 1 H), 7.30–7.38 (m, 1 H), 7.38–7.46 (m, 4 H), 8.12 (d, *J* = 5.5 Hz, 1 H). LCMS: *m/z* 355 [M + H]⁺, *t_R* = 2.50 min.

Biology. Membrane Preparation. CHO cells expressing the human mGlu2 receptor were grown until 80% confluence, washed in ice-cold phosphate buffered saline, and stored at –20 °C until membrane preparation. After thawing, cells were suspended in 50 mM Tris-HCl, pH 7.4, and collected through centrifugation for 10 min at 23500g at 4 °C. Cells were lysed in 5 mM hypotonic Tris-HCl, pH 7.4, and after recentrifugation for 20 min at 30000g at 4 °C, the pellet was homogenized with an Ultra Turrax homogenizer in 50 mM Tris-HCl, pH 7.4. Protein concentrations were measured by the Bio-Rad protein assay using bovine serum albumin as standard.

[³⁵S]GTPγS Binding Assay. For [³⁵S]GTPγS measurements, compound and glutamate were diluted in buffer containing 10 mM HEPES acid, 10 mM HEPES salt, pH 7.4, containing 100 mM NaCl, 3 mM MgCl₂, and 10 μM GDP. Membranes were thawed on ice and diluted in the same buffer, supplemented with 14 μg/mL saponin (final assay concentration of 2 μg/mL saponin). Final assay mixtures contained 7 μg of membrane protein and were preincubated with compound alone (determination of agonist effects) or together with an EC₂₀ concentration (4 μM) of glutamate (determination of PAM effects) for 30 min at 30 °C. [³⁵S]GTPγS was added at a final concentration of 0.1 nM and incubated for another 30 min at 30 °C. Reactions were terminated by rapid filtration through Unifilter-96 GF/B filter plates (PerkinElmer) using a Unifilter-96 Harvester (PerkinElmer). Filters were washed 3 times with ice-cold 10 mM NaH₂PO₄/10 mM Na₂HPO₄, pH 7.4, and filter-bound radioactivity was counted in a Topcount microplate scintillation and luminescence counter from PerkinElmer.

Data Analysis. The concentration–response curves in the presence of added EC₂₅ of mGlu2 agonist glutamate to determine positive allosteric modulation (PAM) were generated using the Prism GraphPad software (Graph Pad Inc., San Diego, CA, U.S.). The curves were fitted to a four-parameter logistic equation $Y = \text{Bottom} + (\text{Top} - \text{Bottom}) / (1 + 10^{(\log EC_{50} - X) \text{Hill slope}})$ allowing determination of EC₅₀ values. The EC₅₀ is the concentration of a compound that causes a half-maximal potentiation of the glutamate response. This is calculated by subtracting the maximal responses of glutamate in the presence of a fully saturating concentration of a positive allosteric modulator from the response of glutamate in the absence of a positive allosteric modulator. The concentration producing the half-maximal effect is then calculated as EC₅₀. The pEC₅₀ values are calculated as the –log EC₅₀ (wherein EC₅₀ is expressed in mol L^{–1}).

Patch Clamp Assay. Experiments were performed using HEK293 cells stably expressing the HERG potassium channel. Cells were grown at 37 °C and 5% CO₂ in culture flasks in MEM medium supplemented with 10% heat-inactivated fetal bovine serum, 1% L-glutamine–penicillin–streptomycin solution, 1% nonessential amino acids (100×), 1% sodium pyruvate (100 mM), and 0.8% Geneticin (50 mg/mL). Before use the cells were subcultured in MEM medium in the absence of 5 mL of L-glutamine–penicillin–streptomycin. For use in the automated patch-clamp system PatchXpress 7000A (Axon Instruments) cells were harvested to obtain cell suspension of single cells. Extracellular solution contained the following (mM): 150 NaCl, 4 KCl, 1 MgCl₂, 1.8 CaCl₂, 10 HEPES, 5 glucose (pH 7.4 with NaOH). Pipette solution contained the following (mM): 120 KCl, 10 HEPES, 5 EGTA, 4 ATP-Mg₂, 2 MgCl₂, 0.5 CaCl₂ (pH 7.2 with KOH). Patch-clamp experiments were performed in the voltage-clamp mode, and whole-cell currents were recorded with an automated

patch-clamp assay utilizing the PatchXpress 7000A system (Axon Instruments). Current signals were amplified and digitized by a Multiclamp amplifier, stored, and analyzed by using the PatchXpress and DataXpress software and Igor 5.0 (Wavemetrics). The holding potential was -80 mV. The HERG current (K^+ -selective outward current) was determined as the maximal tail current at -40 mV after a 2 s depolarization to $+60$ mV. Pulse cycling rate was 15 s. Before each test pulse a short pulse (0.5 s) from the holding potential to -60 mV was given to determine (linear) leak current. After establishment of whole-cell configuration and a stability period, the vehicle was applied for 5 min followed by the test substance at increasing concentrations of 10^{-7} , 3×10^{-7} , and 3×10^{-6} M. Each concentration of the test substance was applied twice. The effect of each concentration was determined after 5 min as an average current of three sequential voltage pulses. To determine the extent of block, the residual current was compared with vehicle pretreatment.

Method for Identification of Main Metabolites. The test compounds were incubated with human and rat liver microsomes at 0.4% final solvent concentration (0.16% DMSO and 0.24% CH_3CN). The study was conducted to identify the main metabolites formed after 0 min (control) and 60 min of incubation time in the presence of NADPH generating system at 37°C . Test concentration of the compound was $5 \mu\text{M}$. Samples were compared to the control incubations in which compound was added at termination. Data were acquired on a Waters UPLC/QToF Premier mass spectrometer using a 10 min generic UPLC method and a generic MSe method. Complementary MS/MS experiments were performed when necessary. An Acquity UPLC C18 ($2.1 \text{ mm} \times 100 \text{ mm}$, $1.8 \mu\text{m}$) column was used. Interpretation of data was performed with Waters Metabolynx software.

Sleep–Wake EEG. Animals, Drug Treatment, and Experimental Procedure. All in vivo experimental procedures were performed according to the applicable European Communities Council Directive of November 24, 1986 (86/609/EEC) and approved by the Animal Care and Use Committee of Janssen Pharmaceutical Companies of Johnson & Johnson and by the local ethical committee.

Male Sprague–Dawley rats (Charles River, France) weighing 250–300 g were used. Animals were chronically implanted with electrodes for recording the cortical electroencephalogram (EEG), electrical neck muscle activity (EMG), and ocular movements (EOG). All animals were housed in individually ventilated cages under environmentally controlled conditions (ambient temperature, 22°C ; humidity, 60%) on a 12 h light/dark cycle (lights on from 12:00 a.m. to 12:00 p.m., illumination intensity of ~ 100 lx). The animals had free access to food and tap water.

The effects of the tested molecule and vehicle on sleep–wake distribution during the lights-on period were investigated in 16 rats ($n = 8$ each group). Two EEG recording sessions were performed: the first recording session started at 13:30 h and lasted 20 h following oral administration of saline. The second recording session was performed during the same consecutive circadian time and for the same duration following administration of either vehicle (20% CD + 2H2T) or tested compound.

Sleep polysomnographic variables were determined offline as described elsewhere using a sleep stages analyzer, scoring each 2 s epoch before averaging stages over 30 min periods. Sleep–wake state classifications were assigned based upon combination of dynamics of five EEG frequency domains, integrated EMG, EOG, and body activity level: active wake (AW); passive wake (PW); intermediate stage (pre-REM transients); rapid eye movement sleep (REM); light non-REM sleep (ISWS); deep non-REM sleep (dSWS). Different sleep–wake parameters were investigated over 20 h postadministration, and time spent in each vigilance state, sleep parameters, latencies for first REM sleep period and the number of transitions between states were determined.

Statistical Analysis. Time spent in each vigilance state (AW, PW, ISWS, dSWS, IS, and REMS) was expressed as a percentage of the recording period. A statistical analysis of the obtained data was carried out by a nonparametric analysis of variance of each 30 min period,

followed by a Wilcoxon–Mann–Whitney rank sum test of comparisons with the control group.

Phencyclidine (PCP) Induced Hyperlocomotion in Mice. Male NMRI mice (Charles River, France or Germany) were housed 5 per cage and kept under a 12 h light/dark cycle under constant temperature and humidity conditions. All experimental procedures were performed in full compliance with the European legislation governing the protection of animals used in scientific research. Phencyclidine (PCP) was purchased from Sigma-Aldrich (France). Nonhabituated animals were treated with the vehicle, or **20**, and immediately challenged with either PCP (5.0 mg/kg, sc) or vehicle and individually placed into open-fields for a 30 min period. The distance traveled by animals was measured using video tracking and computerized analysis systems (Ethovision XT video tracking system, version 3.1; Noldus, Wageningen, The Netherlands). Averaged activity in solvent-treated control mice was 11096 ± 3612 counts (mean \pm SD; $n = 2334$). The criterion for drug-induced inhibition of hyperlocomotion was the following: total distance of < 5500 counts (4.9% false positives). ED_{50} values (the dose inducing 50% responders to this criterion) and corresponding 95% confidence limits were determined according to the modified Spearman–Kaerber estimate, using theoretical probabilities instead of empirical ones.⁵⁹ This modification allows the determination of the ED_{50} and its confidence interval as a function of the slope of the log dose–response curve.⁶⁰

■ ASSOCIATED CONTENT

📄 Supporting Information

LCMS methods for the characterization of intermediate and final compounds. This material is available free of charge via the Internet at <http://pubs.acs.org>.

■ AUTHOR INFORMATION

✉ Corresponding Author

*Phone: +34 925 245767. Fax: +34 925 245771. E-mail: jcid@its.jnj.com.

📄 Notes

The authors declare no competing financial interest.

■ ACKNOWLEDGMENTS

The authors thank collaborators from Addex Therapeutics and the members of the purification and analysis group and the biology and in vitro metabolism team from Janssen R&D.

■ ABBREVIATIONS USED

ADMET, absorption, distribution, metabolism, excretion, and toxicity; AMPA, α -amino-3-hydroxy-5-methyl-4-isoxazolepropionic acid; BBB, blood–brain barrier; AUC, area under the curve; AW, active wake; CNS, central nervous system; CyPr, cyclopropyl; DMS-IV, diagnostic statistical manual of mental disorders volume IV; dSWS, deep non-REM sleep; EEG, electroencephalogram; EMG, electrical neck muscle activity; EOG, ocular movement; GABA, γ -aminobutyric acid; GPCR, G-protein-coupled receptor; HLM, human liver microsome; HP- β -CD, 2-hydroxypropyl- β -cyclodextrin; HTS, high throughput screening; imidazo[1,2-*a*]pyridine; iv, intravenous; LAD, lowest active dose; LE, ligand efficiency; LELP, lipophilicity-corrected ligand efficiency; LLE, lipophilic ligand efficiency; LMA, locomotor activity; mGlu2, metabotropic glutamate 2; ISWS, light non-REM sleep; MW, molecular weight; ND, not determined; nm, not measurable; NMDA, *N*-methyl-D-aspartate; NOEL, no effect level; nt, not tested; PAM, positive allosteric modulator; PCP, phencyclidine; PK, pharmacokinetics; PW, passive wake; SAR, structure–activity relationship; SEM, standard error of mean; po, oral; REM, rapid eye movement; RLM, rat liver microsome; ROL,

REM sleep onset latency; sc, subcutaneous; SD, standard deviation; sw-EEG, sleep–wake electroencephalogram; TPSA, total polar surface area; triazolopyridine, 1,2,4-triazolo[4,3-*a*]pyridine

REFERENCES

- (1) Niswender, C. M.; Conn, J. P. Metabotropic glutamate receptors: physiology, pharmacology, and disease. *Annu. Rev. Pharmacol. Toxicol.* **2010**, *50*, 295–322.
- (2) Pilc, A.; Chaki, S.; Nowak, G.; Witkin, J. M. Mood disorders: regulation by metabotropic glutamate receptors. *Biochem. Pharmacol.* **2008**, *75*, 997–1006.
- (3) Lüscher, C.; Huber, K. M. Group 1 mGluR-dependent synaptic long-term depression: mechanisms and implications for circuitry and disease. *Neuron* **2010**, *65*, 445–459.
- (4) Vinson, P. N.; Conn, P. J. Metabotropic glutamate receptors as therapeutic targets for schizophrenia. *Neuropharmacology* **2012**, *62*, 1461–1472.
- (5) Chiechio, S.; Nicoletti, F. Metabotropic glutamate receptors and the control of chronic pain. *Curr. Opin. Pharmacol.* **2012**, *12*, 28–34.
- (6) Foster, O. M. Metabotropic glutamate receptor ligands as potential therapeutics for addiction. *Curr. Drug Abuse Rev.* **2009**, *2*, 83–98.
- (7) Johnson, K. A.; Conn, P. J.; Niswender, C. M. Glutamate receptors as therapeutic targets for Parkinson's disease. *CNS Neurol. Disord.: Drug Targets* **2009**, *8*, 475–491.
- (8) Watkins, J. C. L-Glutamate as a central neurotransmitter: looking back. *Biochem. Soc. Trans.* **2000**, *28*, 297–310.
- (9) Kew, J. N. C.; Kemp, J. A. Ionotropic and metabotropic glutamate receptor structure and pharmacology. *Psychopharmacology* **2005**, *179*, 4–29.
- (10) Huang, S.; Cao, J.; Jiang, M.; Labesse, G.; Liu, J.; Pin, J.-P.; Rondard, P. Interdomain movements in metabotropic glutamate receptor activation. *Proc. Natl. Acad. Sci. U.S.A.* **2011**, *108*, 15480–15485.
- (11) Pin, J. P.; Galvez, T.; Prezeau, L. Evolution, structure, and activation mechanism of family 3/C G-protein-coupled receptors. *Pharmacol. Ther.* **2003**, *98*, 325–354.
- (12) Brauner-Osborne, H.; Wellendorph, P.; Jensen, A. A. Structure, pharmacology and therapeutic prospects of family C G-protein coupled receptors. *Curr. Drug Targets* **2007**, *8*, 169–184.
- (13) Cartmell, J.; Schoepp, D. D. Regulation of neurotransmitter release by metabotropic glutamate receptors. *J. Neurochem.* **2000**, *75*, 889–907.
- (14) Ohishi, H.; Shigemoto, R.; Nakanishi, S.; Mizuno, N. Distribution of the messenger RNA for metabotropic glutamate receptor, mGlu2, in the central nervous system of the rat. *Neuroscience* **1993**, *53*, 1009–1018.
- (15) Richards, G.; Messer, J.; Malherbe, P.; Pink, R.; Brockhaus, M.; Stadler, H.; Wichmann, J.; Schaffhauser, H. J.; Mutel, V. Distribution and abundance of metabotropic glutamate receptor subtype 2 in rat brain revealed by [³H]LY354740 binding in vitro and quantitative radioautography: correlation with the sites of synthesis, expression, and agonist stimulation of [³⁵S]GTPγS binding. *J. Comp. Neurol.* **2005**, *487*, 15–27.
- (16) Gu, G.; Lorrain, D. S.; Wei, H.; Cole, R. L.; Zhang, X.; Daggett, L. P.; Schaffhauser, H. J.; Bristow, L. J.; Lechner, S. M. Distribution of metabotropic glutamate 2 and 3 receptors in the rat forebrain: implication in emotional responses and central disinhibition. *Brain Res.* **2008**, *1197*, 47–62.
- (17) Ghose, S.; Gleason, K. A.; Potts, B. W.; Lewis-Amezcu, K.; Tamminga, C. A. Differential expression of metabotropic glutamate receptors 2 and 3 in schizophrenia: a mechanism for antipsychotic drug action? *Am. J. Psychiatry* **2009**, *166*, 812–820.
- (18) Shigeyuki, C.; Hirohiko, H. Targeting of metabotropic glutamate receptors for the treatment of schizophrenia. *Curr. Pharm. Des.* **2011**, *17*, 94–102.
- (19) Monn, J. A.; Valli, M. J.; Massey, S. M.; Wright, R. A.; Salhoff, C. R.; Johnson, B. G.; Howe, T.; Alt, C. A.; Rhodes, G. A.; Robey, R. L.; Griffey, K. R.; Tizzano, J. P.; Kallman, M. J.; Helton, D. R.; Schoepp, D. D. Design, synthesis, and pharmacological characterization of (+)-2-aminobicyclo[3.1.0]hexane-2,6-dicarboxylic acid (LY354740): a potent, selective, and orally active group 2 metabotropic glutamate receptor agonist possessing anticonvulsant and anxiolytic properties. *J. Med. Chem.* **1997**, *40*, 528–537.
- (20) Swanson, C. J.; Bures, M.; Johnson, M. P.; Linden, A. M.; Monn, J. A.; Schoepp, D. D. Glutamate receptors as novel targets for anxiety and stress disorders. *Nat. Rev. Drug Discovery* **2005**, *4*, 131–144.
- (21) Fell, M. J.; McKinzie, D. L.; Monn, J. A.; Svensson, K. A. Group II metabotropic glutamate receptor agonists and positive allosteric modulators as novel treatments for schizophrenia. *Neuropharmacology* **2012**, *62*, 1473–1483.
- (22) Patil, S. T.; Zhang, L.; Martenyi, F.; Lowe, S. L.; Jackson, K. A.; Andreev, B. V.; Avedisova, A. S.; Bardenstein, L. M.; Gurovich, I. Y.; Morozova, M. A.; Mosolov, S. N.; Neznanov, N. G.; Reznik, A. M.; Smulevich, A. B.; Tochilov, V. A.; Johnson, B. G.; Monn, J. A.; Schoepp, D. D. Activation of mGlu2/3 receptors as a new approach to treat schizophrenia: a randomized phase 2 clinical trial. *Nat. Med.* **2007**, *13*, 1102–1107.
- (23) During the preparation of this manuscript Eli Lilly and Company announced in a press release (August 29, 2012) the decision to stop the clinical studies investigating LY2140023 for the treatment of patients suffering from schizophrenia. The press release mentioned that the decision was made after a recently conducted independent futility analysis concluded that HBBN, the second of Lilly's two pivotal studies, was unlikely to be positive in its primary efficacy endpoint if enrolled to completion. The decision was not based on any safety signals. <https://investor.lilly.com/releaseDetail.cfm?ReleaseID=703018>.
- (24) Pin, J. P.; Parmentier, M.-L.; Prezeau, L. Positive allosteric modulators for γ -aminobutyric acid_B receptors open new routes for the development of drugs targeting family 3 G-protein-coupled receptors. *Mol. Pharmacol.* **2001**, *60*, 881–884.
- (25) Gjoni, T.; Urwyler, S. Receptor activation involving positive allosteric modulation, unlike full agonism, does not result in GABA_B receptor desensitization. *Neuropharmacology* **2008**, *55*, 1293–1299.
- (26) Urwyler, S. Allosteric modulation of family C G-protein-coupled receptors: from molecular insights to therapeutic perspectives. *Pharmacol. Rev.* **2011**, *63*, 59–126.
- (27) Trabanco, A. A.; Cid, J. M.; Lavreysen, H.; Macdonald, G. J.; Tresadern, G. Progress in the development of positive allosteric modulators of the metabotropic glutamate receptor 2. *Curr. Med. Chem.* **2011**, *18*, 47–68.
- (28) Trabanco, A. A.; Duvey, G.; Cid, J. M.; Macdonald, G. J.; Cluzeau, P.; Nhem, V.; Furnari, R.; Behaj, N.; Poulain, G.; Finn, T.; Lavreysen, H.; Poli, S.; Raux, A.; Thollon, Y.; Poirier, N.; D'Addona, D.; Andrés, J. I.; Lutjens, R.; Le Poul, E.; Imogai, H.; Rocher, J.-P. New positive allosteric modulators of the metabotropic glutamate receptor 2 (mGluR2): identification and synthesis of N-propyl-8-chloro-6-substituted isoquinolones. *Bioorg. Med. Chem. Lett.* **2011**, *21*, 971–976.
- (29) Trabanco, A. A.; Duvey, G.; Cid, J. M.; Macdonald, G. J.; Cluzeau, P.; Nhem, V.; Furnari, R.; Behaj, N.; Poulain, G.; Finn, T.; Poli, S.; Lavreysen, H.; Raux, A.; Thollon, Y.; Poirier, N.; D'Addona, D.; Andrés, J. I.; Lutjens, R.; Le Poul, E.; Imogai, H.; Rocher, J.-P. New positive allosteric modulators of the metabotropic glutamate receptor 2 (mGluR2): identification and synthesis of N-propyl-5-substituted isoquinolones. *Med. Chem. Commun.* **2011**, *2*, 132–139.
- (30) Cid, J. M.; Duvey, G.; Cluzeau, P.; Nhem, V.; Macary, K.; Raux, A.; Poirier, N.; Muller, J.; Bolea, C.; Finn, T.; Urios, I.; Epping-Jordan, M.; Chamelot, E.; Derouet, F.; Girard, F.; Macdonald, G. J.; Vega, J. A.; de Lucas, A. I.; Matesanz, E.; Lavreysen, H.; Linares, M. L.; Oehlich, D.; Oyarzábal, J.; Tresadern, G.; Trabanco, A. A.; Andrés, J. I.; Le Poul, E.; Imogai, H.; Lutjens, R.; Rocher, J.-P. Discovery of 1,5-disubstituted pyridones: a new class of positive allosteric modulators of the metabotropic glutamate 2 receptor. *ACS Chem. Neurosci.* **2010**, *1*, 788–795.

- (31) Imogai, H. J.; Cid-Nuñez, J. M.; Duvey, G. A. J.; Bolea, C. M.; Nhem, V.; Finn, T. P.; Le Poul, E. C.; Rocher, J.-P. F. C.; Lutjens, R. J. Novel Pyridinone Derivatives and Their Preparation, Pharmaceutical Compositions, and Use as Positive Allosteric Modulators of mGluR2-Receptors for Treatment of Various Neurological and Psychiatric Disorders. WO2006030032 A1, 2006.
- (32) Cid, J. M.; Duvey, G.; Tresadern, G.; Nhem, V.; Funary, R.; Cluzeau, P.; Vega, J. A.; de Lucas, A. I.; Matesanz, E.; Alonso, J. M.; Linares, M. L.; Andrés, J. I.; Poli, S.; Lutjens, R.; Imogai, H.; Rocher, J.-P.; Macdonald, G. J.; Oehlich, D.; Lavreysen, H.; Ahnaou, A.; Drinkenburg, W.; Mackie, C.; Trabanco, A. A. Discovery of 1,4-disubstituted 3-cyano-2-pyridones: a new class of positive allosteric modulators of the metabotropic glutamate 2 receptor. *J. Med. Chem.* **2012**, *55*, 2388–2405.
- (33) Cid-Nuñez, J. M.; Trabanco-Suárez, A. A.; Macdonald, G. J.; Duvey, G. A. J.; Lutjens, R. J. Preparation of 3-Cyano-4-(4-tetrahydropyran-phenyl)pyridin-2-one Derivatives as Positive mGluR2 Receptor Modulators. WO 2008107481 A1, 2008.
- (34) Imogai, H. I.; Cid-Nuñez, J. M.; Andrés-Gil, J. I.; Trabanco-Suárez, A. A.; Oyarzábal-Santamarina, J.; Dautzenberg, F. M.; Macdonald, G. J.; Pullan, S. E.; Lutjens, R. J.; Duvey, G. A. J.; Nhem, V.; Finn, T. P.; Melikyan, G. 1,4-Disubstituted 3-Cyanopyridone Derivatives and Their Use as Positive Allosteric Modulators of mGlu2-Receptors and Their Preparation. WO2007104783 A2, 2007.
- (35) Tresadern, G.; Cid, J. M.; Macdonald, G. J.; Vega, J. A.; de Lucas, A. I.; García, A.; Matesanz, E.; Linares, M. L.; Oehlich, D.; Lavreysen, H.; Biesmans, I.; Trabanco, A. A. Scaffold hopping from pyridones to imidazo[1,2-*a*]pyridines. New positive allosteric modulators of metabotropic glutamate 2 receptor. *Bioorg. Med. Chem. Lett.* **2010**, *20*, 175–179.
- (36) Trabanco, A. A.; Tresadern, G.; Macdonald, G. J.; Vega, J. A.; de Lucas, A. I.; Matesanz, E.; García, A.; Linares, M. L.; Alonso de Diego, S. A.; Alonso, J. M.; Oehlich, D.; Ahnaou, A.; Drinkenburg, W.; Mackie, C.; Andres, J. I.; Lavreysen, H.; Cid, J. M. Imidazo[1,2-*a*]pyridines: orally active positive allosteric modulators of the metabotropic glutamate 2 receptor. *J. Med. Chem.* **2012**, *55*, 2688–2701.
- (37) Cid-Nuñez, J. M.; Trabanco-Suárez, A. A.; Macdonald, G. J. Preparation of Indole and Benzoxazine Derivatives as Modulators of Metabotropic Glutamate Receptors for Treating Neurological and Psychiatric Disorders. WO 2010060589 A1, 2010.
- (38) Trabanco-Suárez, A. A.; Tresadern, G. J.; Vega-Ramiro, J. A.; Cid-Nuñez, J. M. Preparation of Imidazopyridine Derivatives for Use as mGluR2 Receptor Modulators. WO2009062676 A2, 2009.
- (39) Cid-Nuñez, J. M.; Oehlich, D.; Trabanco-Suárez, A. A.; Tresadern, G. J.; Vega-Ramiro, J. A.; Macdonald, G. J. 1,2,4-Triazolo[4,3-*a*]pyridine Derivatives and Their Use for the Treatment or Prevention of Neurological Disorders. WO2010130424 A1, 2010.
- (40) Cid-Nuñez, J. M.; De Lucas-Olivares, A. I.; Trabanco-Suárez, A. A.; Macdonald, G. J. 7-Aryl-1,2,4-triazolo[4,3-*a*]pyridine Derivatives and Their Use as Positive Allosteric Modulators of mGluR2 Receptors. WO2010130423 A1, 2010.
- (41) Cid-Nuñez, J. M.; De Lucas-Olivares, A. I.; Trabanco-Suárez, A. A.; Macdonald, G. J. 1,2,4-Triazolo[4,3-*a*]pyridine Derivatives and Their Use as Positive Allosteric Modulators of mGluR2 Receptors. WO2010130422 A1, 2010.
- (42) The in vitro [³⁵S]GTPγS assay provides two measures of compound activity: pEC₅₀, which is defined as the negative logarithm of the concentration at which half-maximal potentiation of glutamate is reached, and the maximal increase in observed glutamate response, the % E_{MAX}.
- (43) Compound **20** shifts the concentration–response curve of glutamate to the left, increasing the potency of glutamate up to ~25-fold.
- (44) Gleeson, M. P. Generation of a set of simple, interpretable ADMET rules of thumb. *J. Med. Chem.* **2008**, *51*, 817–834.
- (45) Leeson, P. D.; Springthorpe, B. The influence of drug-like concepts on decision-making in medicinal chemistry. *Nat. Rev. Drug Discovery* **2007**, *6*, 881–890.
- (46) Keseru, G. M.; Makara, G. M. The influence of lead discovery strategies on the properties of drug candidates. *Nat. Rev. Drug Discovery* **2009**, *8*, 203–212.
- (47) Tarcsay, A.; Nyiri, K.; Keseru, G. M. Impact of lipophilic efficiency on compound quality. *J. Med. Chem.* **2012**, *55*, 1252–1260.
- (48) Molecule **20** had a calculated (ACD, version 12.0) log *D* at pH 7.4 of 2.65, subtracted from the in vitro potency of 15 nM (pEC₅₀ of 7.82), and yielded an LLE of 5.2. However, some caution may be needed, as the experimental log *P* was 4.4 (pH 7.0, Table 5), suggesting a discrepancy between experiment and theory in this case.
- (49) The CEREP selectivity screen was performed on the following targets: SHT_{1A}, SHT_{2A}, SHT₃, SHT_{5A}, SHT₆, SHT₇, A₁, A_{2A}, A₃, AT₁, β₁, BK₂, CCKA, CCR₁, D₁, D₂, DAT, ETA, GAL₂, H₁, H₂, IL_{8B}, CXCR₂, M₁, M₂, M₃, MC₄, NET, NK₂, NK₃, NPY₁, NPY₂, NT₁, OP₁, OP₃, ORL₁, V_{1A}, VIP, SST, SHT_{1B}, α₁, α₂, BZD, CaCH, CICH, GABA, KCH, NaCH, SKCaCH.
- (50) Lopez-Rodriguez, F.; Medina-Ceja, L.; Wilson, C. L.; Jhung, D.; Morales-Villagram, A. Changes in extracellular glutamate levels in rat orbitofrontal cortex during sleep and wakefulness. *Arch. Med. Res.* **2007**, *38*, 52–55.
- (51) Ahnaou, A.; Dautzenberg, F. M.; Geys, H.; Imogai, H.; Gibelin, A.; Moechars, D.; Steckler, T.; Drinkenburg, W. H. I. M. Modulation of group II metabotropic glutamate receptor (mGlu2) elicits common changes in rat and mice sleep–wake architecture. *Eur. J. Pharmacol.* **2009**, *603*, 62–72.
- (52) Feinberg, I.; Schoepp, D. D.; Hsieh, K.-C.; Darchia, N.; Campbell, I. G. The metabotropic glutamate (mGLU)2/3 receptor antagonist LY341495 [2S-2-amino-2-(1S,2S-2-carboxycyclopropyl-1-yl)-3-(xanth-9-yl)propanoic acid] stimulates waking and fast electroencephalogram power and blocks the effects of the mGLU2/3 receptor agonist LY379268 [(–)-2-oxa-4-aminobicyclo[3.1.0]hexane-4,6-dicarboxylate] in rats. *J. Pharmacol. Exp. Ther.* **2005**, *312*, 826–833.
- (53) Fell, M. J.; Witkin, J. M.; Falcone, J. F.; Katner, J. S.; Perry, K. W.; Hart, J.; Rorick-Kehn, L.; Overshiner, C. D.; Rasmussen, K.; Chaney, S. F.; Benvenaga, M. J.; Deanna, X. L.; Marlow, L.; Thompson, L. K.; Luecke, S. K.; Wafford, K. A.; Seidel, W. F.; Edgar, D. M.; Quets, A. T.; Felder, C. C.; Wang, X.; Heinz, B. A.; Nikolayev, A.; Kuo, M.-S.; Mayhugh, D.; Khilevich, A.; Zhang, D.; Ebert, P. J.; Eckstein, J. A.; Ackermann, B. L.; Swanson, S. P.; Catlow, J. T.; Dean, R. A.; Jackson, K.; Tauscher-Wisniewski, S.; Marek, G. J.; Schkeryantz, J. M.; Svensson, K. A. N-(4-((2-(Trifluoromethyl)-3-hydroxy-4-(isobutyryl)-phenoxy)methyl)benzyl)-1-methyl-1H-imidazole-4-carboxamide (THIIC), a novel metabotropic glutamate 2 potentiator with potential anxiolytic/antidepressant properties: in vivo profiling suggests a link between behavioral and central nervous system neurochemical changes. *J. Pharmacol. Exp. Ther.* **2011**, *336*, 165–177.
- (54) Siok, C. J.; Cogan, S. M.; Shifflett, L. B.; Doran, A. C.; Kocsis, B.; Hajós, M. Comparative analysis of the neurophysiological profile of group II metabotropic glutamate receptor activators and diazepam: effects on hippocampal and cortical EEG patterns in rats. *Neuropharmacology* **2012**, *62*, 226–236.
- (55) Free plasma concentrations were calculated by multiplying total plasma concentrations with plasma free fraction (plasma protein binding (%) of 0.35).
- (56) Gleason, S. D.; Shannon, H. E. Blockade of phencyclidine-induced hyperlocomotion by olanzapine, clozapine and serotonin receptor subtype selective antagonists in mice. *Psychopharmacology* **1997**, *129*, 79–84.
- (57) Affinity of JNJ42153605 for the mGlu2 receptor allosteric binding site was evaluated using a radioligand structurally related analogue developed in house. A manuscript describing the synthesis, in vitro and in vivo characterization of this radioligand, and the development of an in vivo assay to measure mGlu2 receptor occupancy is in preparation and will be reported elsewhere.
- (58) An internal report on the method is available upon request: Beerens, D. In Vitro Bacterial Reverse Mutation (Plate Incorporation) Assay with JNJ42153605-AAA in *Salmonella typhimurium* TA98; May 2009.

(59) Tsutakawa, R. K. Statistical Methods in Bioassay. Estimation of Relative Potency from Quantal Responses. In *Encyclopaedia of Statistical Science*; Kotz, S., Jonhson, N. L., Eds.; Wiley: New York, 1982.

(60) An internal report on the method is available upon request: Lewi, P. J.; Niemegeers, C. J. E.; Gypen, L. M. J. First Hand Estimation of the Median Effective Dose (ED_{50}) and Its Confidence Interval, Assuming a Linear Log Dose-Response Function. Internal Report N123705/1; Department of Global Medical and Scientific Information, Johnson & Johnson Pharmaceutical Research and Development, a Division of Janssen Pharmaceutica, Turnhoutseweg 30, B-2340 Beerse, Belgium, 1997.